Ewsa-dependent regulation of Runx2 during zebrafish skeletogenesis

By

Luke William Wenger

Submitted to the graduate degree program in Molecular, Cellular, and Developmental Biology and the Graduate Faculty of the University of Kansas in partial fulfillment of the requirements for the degree of Master of Arts.

_____

Chairperson Dr. Mizuki Azuma

_____

Dr. Kristi Neufeld

_____

Dr. Stuart Macdonald

Date Defended: 02-May, 2016

The Thesis Committee for Luke William Wenger

certifies that this is the approved version of the following thesis:

Ewsa-dependent regulation of Runx2 during zebrafish skeletogenesis and axis development

_____

Chairperson Dr. Mizuki Azuma

Date approved: 10-May, 2016

ABSTRACT

Ewing's sarcoma is the second most common malignant bone cancer found in adolescents, and the genetic hallmark of this disease is the presence of the aberrant chimeric fusion protein EWS/FLI1. This fusion is induced by the t(11; 22) chromosomal translocation of *EWS* and *FLI1*, and is the most prominent and common characteristic of Ewing sarcoma tumors found in approximately 85-90% of reported cases. EWS/FLI1 has been shown to directly bind to and inhibit the function of endogenous EWS in a dominant manner. In this study, we seek to increase our understanding of the role of endogenous EWS during development and skeletogenesis to gain insight into the pathogenesis of the disease. Previously, we demonstrated the role of a zebrafish EWS homolog Ewsa by analyzing the phenotype of a maternal zygotic homozygous *ewsa/ewsa* mutant line (MZ *ewsa/ewsa*) of zebrafish null for Ewsa protein. Prehypertrophic chondrocytes of Meckel's cartilage in 4dpf MZ *ewsa/ewsa* mutants fail to completely differentiate into hypertrophic chondrocytes, followed by structural defects in craniofacial bones (dentary and basihyal bones) at the adult stage. Based on these results, we sought to understand EWS's involvement in skeletogenesis by asking if Ewsa regulates activity of critical transcription factors involved in chondrocyte development. We have previously shown that Ewsa directs chondrocyte differentiation through modulation of chondrogenesis master transcription factor Sox9. Runx2 is also known to play a critical role in differentiation of both chondrocytes and osteoblasts, so we have addressed whether and how Ewsa regulates Runx2 expression and transcriptional activity. We discovered that Runx2 protein expression dramatically increases in craniofacial chondrocytes of 4-6dpf MZ *ewsa/ewsa* compared to wt/wt embryos. We have also observed premature mineralization in MZ *ewsa/ewsa* embryos at 6dpf and 10dpf. MZ *ewsa/ewsa* fish also display a decrease in expression of *collagen10a1*, a hypertrophic-specific Runx2 target gene. These data together suggests that Ewsa regulates Runx2 expression and transcriptional activity during chondrogenesis and regulates mineralization of these domains. Additionally, our lab has previously discovered that adult MZ *ewsa/ewsa* fish display aberrant

curved spines. Based on these results we asked how Ewsa is involved in the formation of the axial skeleton. Since Collagen2a1 is a critical component of notochord development as both a precursor to intervertebral disc (IVD) formation and as a component of notochord sheath extracellular matrix (ECM) we have previously asked if Ewsa regulates the *collagen2a1a* gene. Ewsa interacts with the *col2a1a* gene and col2a1 is upregulated in the notochord MZ *ewsa/ewsa* fish which suggests that the notochord sheath ECM is misregulated in mutant fish. Additionally, our analysis also revealed that notochord cells have failed to intercalate 5-10dpf and remain in a single layer. Based on our previous data and the data in this report, we hypothesize that Ewsa regulates axis development through regulation of *collagen2a1* expression, which in turn allows for normal notochord sheath ECM distribution, which in turn allows for notochord cell intercalation and later IVD and vertebral body formation. This is the first *in vivo* evidence for regulation of RUNX2 by EWS during chondrogenesis and axial skeleton development.

ACKNOWLEDGMENTS

This sure has been an incredible journey. Thank you so much to everyone who has made this experience an amazing one. First and foremost, I would like to thank my advisor, Dr. Mizuki Azuma, who trained me to work like a scientist, think critically as a scientist, and question everything as well as provide me with valuable life advice I will never forget. Thank you also for always ensuring the lab is supplied with both coffee and cookies, without which I would not have survived. Thank you Mizuki! I would also like to thank my committee members, Dr. Kristi Neufeld and Dr. Stuart Macdonald, for their support and guidance throughout this process. I would also like to thank Dr. Yoshiaki Azuma and his lab for helpful discussion, use of reagents and equipment, and their peace offerings of chocolate.

Thank you to everyone whom I have had the fortune to work with in the Azuma lab here at KU. I have honestly no idea what you will do without me; probably enjoy having an excess of leftover food? Thank you to Hyewon Park, for her technical assistance and helpful discussion. Thank you to my fellow grad students Seth Lewin, chef, artist, and hunter extraordinaire, and Sudeep Shakya, my ping-pong sensei, for putting up with all my shenanigans. Thank you to the undergrad Justin Mehojah for allowing me to brainwash him with an interest in zebrafish and developmental biology.

An extra special thanks to Seth Lewin, who has been not only a fantastic colleague to discuss ideas and science with, but one of the greatest friends, chef, confidante, and labmate one could ask for, if not the greatest.

In my short time here at KU I have found a profound admiration for the process of science and the pursuit of curiosity. I found a fantastic lab to further my scientific training in, a deep respect for my fellow scientists, a love of teaching, and a newfound interest in developmental biology. Thank you to the Massman Family Ewing Sarcoma Research Fund and the National Institutes of Health (grants no. P20GM103418, P20GM103638) for funding. Finally, thank you to my family for their unconditional love and support throughout this process since t=0.

Table of Contents

INTRODUCTION

EWS (*EWSR1, Ewing sarcoma breakpoint region 1*) is a gene that was originally discovered in Ewing sarcoma (ES), the second most common bone cancer found in children and young adults. The hallmark of this disease is the presence of an aberrant fusion gene encoding the N-terminal transcriptional activation domain of *EWS* and the C-terminal domain of an ETS transcription factor, formed by a chromosomal translocation [1]. The most common fusion gene reported, *EWS/FLI1,* is known to drive aberrant transcription of target genes compared to cells not expressing *EWS/FLI1* [2-4] and induces altered splicing events [5, 6]. EWS/FLI1 has also been shown to interact directly with EWS to inhibit its endogenous function in a dominant negative manner [7], and human cells with depleted EWS display mitotic defects, a phenotype similar to what is seen in cells expressing EWS/FLI1 [8]. This raises the possibility that EWS function may be inhibited in ES skeletal tumors due to the dominant activity of EWS/FLI1 on EWS. Therefore, elucidating the endogenous role of EWS in skeletal development is essential to understanding the pathogenesis of ES.

Evidence for a role of EWS in skeletal development was first demonstrated using EWS knockout mice, which display smaller size compared to wild-type littermates and decreased density of long bones and 90% postnatal lethality [9]. This study demonstrated that EWS plays a critical role during development, but the exact mechanism of EWS during skeletogenesis and long bone formation is not explained. The formation of long bones, the site of ES, develops through endochondral ossification (Fig. 1). The other processes of bone formation is intramembranous ossification, which occurs by direct ossification of mesenchymal precursors giving rise to bone. Endochondral ossification begins with the condensation of mesenchymal precursor cells. These condensations are first driven to the cartilage lineage and differentiate into proliferating chondrocytes via SOX9 (SRY, (Sex Determining Region Y) - box 9) activity [10]. Proliferating chondrocytes then undergo tightly controlled changes in gene expression and morphology to promote progression into intermediate prehypertrophic cells before differentiating into

hypertrophic cells, followed by mineralization of the extracellular matrix. The hypertrophic chondrocytes then secrete factors to induce angiogenesis which brings in osteoblasts and then undergo cell death before being replaced by bone deposited by osteoblasts.

To increase our understanding of the *in vivo* role of EWS, we utilized zebrafish as a model. The two zebrafish orthologues of human EWS were first described as *ewsr1a* (*ewsa*) and *ewsr1b* (*ewsb*) [11]. Depletion of *ewsa* and *ewsb* via morpholino injection at the one-cell stage contributed to mitotic defects induced via multipolar and abnormal spindles, and embryos depleted of *ewsa* and *ewsb* also displayed a reduced number of proneural cells due to p53-mediated apoptosis in the central nervous system and embryonic lethality by 5dpf [11]. These initial results describe the essential role of *ewsa* and *ewsb* during development. To study the role of EWS during skeletogenesis, we obtained a maternal zygotic (MZ) *ewsa*/ewsa zebrafish line null for Ewsa. Zebrafish depleted of *ewsb* did not survive to adulthood. We have found that MZ *ewsa/ewsa* mutant fish display defects in cartilage structures including impaired differentiation of chondrocytes and aberrant angle of Meckel's cartilage and palatoquadrate structures, emphasizing the role of EWS in skeletogenesis [12]. To explain this mechanism, in this same report [12], we demonstrated a role for EWS in chondrocyte development to regulate SOX9.

The other essential transcription factor required for chondrogenesis is the skeletogenesis master transcription factor RUNX2 (Runt-related transcription factor 2). SOX9 is essential for driving cells into the chondrocyte lineage and preventing hypertrophy, but maturation of chondrocytes to hypertrophic chondrocytes is driven by RUNX2 and inhibited by SOX9 through direct inhibition of RUNX2 by SOX9 [13-15]. For the correct gene expression changes that take place during chondrocyte differentiation to occur, SOX9 activity must be inhibited and RUNX2 activity must be promoted. In RUNX2-deficient mice, the skeletal structures consist of only resting and proliferating cartilage [16-18]. These mice also display postnatal lethality due to a complete lack of ossification due to the absence of mature osteoblasts [19] providing further evidence for the importance of RUNX2 during both chondrogenesis and skeletogenesis. Since Ewing sarcoma

occurs in skeletal tissue, we need to increase our understanding of the molecular mechanisms by which EWS directs chondrocyte maturation. Loss of Ewsa in fish contributes to defects in cartilage structures, and since Runx2 is required to drive cartilage differentiation, we seek to determine if regulation of RUNX2 occurs in zebrafish null for Ewsa. We then ask specifically how Ewsa regulates Runx2 and if this is done by controlling Runx2 mRNA transcription, Runx2 protein translation, and/or transcriptional activity of Runx2. We investigate how Ewsa regulates Runx2 during chondrogenesis, and how this regulation influences the transcriptional profile of chondrocytes during differentiation.

During this study we also aimed to elucidate the function of Ewsa in axial skeletal formation. The axial skeleton is derived from the notochord, a critical structural component and signaling center in zebrafish. Preceding axis formation, the notochord must undergo vacuolization followed by secretion of extracellular matrix (ECM) proteins, notably type II collagen, to form the sheath surrounding the notochord. [20-22]. Also, the formation of the ECM is critical for proper development of the notochord and spine because notochord cells provide pressure on the sheath for support and provide the notochord with its structural properties [23]. The sheath itself is composed of both condensed and non-condensed areas. The condensed areas form the nucleus pulposus cells and the non-condensed areas give rise to sclerotome cells, the precursor of vertebral bodies [24]. Notochord cells located in vertebral bodies are then removed and relocate to intervertebral regions where they form the nucleus pulposus cells which then give rise to the intervertebral discs (IVD) [25, 26]. Sclerotome cells migrate around the notochord and undergo endochondral ossification to form the vertebrae [27]. Adult MZ *ewsa/ewsa* fish in our lab display aberrant curved spines likely due to a defect in IVD formation, impaired differentiation of nucleus pulposus cells, and overexpression of type II collagen in the notochord and ECM. These mutants also display premature vertebrae formation compared to wild-type. In Collagen II-deficient mice, the notochord persists as a rod-like structure in vertebral bodies until birth [28] providing evidence of the critical importance of Collagen II during axis formation. Our previous data suggest that

Ewsa is critical for formation of the axial skeleton possibly through regulation of type II collagen. It is unknown, however, how Ewsa-dependent regulation of the notochord sheath and ECM contributes to the development of the notochord. In this study we aim to elucidate the first steps of the mechanism underlying how the formation of the notochord is regulated by Ewsa to ultimately form the skeletal axis. Together, in this report we investigate how Ewsa regulates chondrogenesis through regulation of Runx2 expression as well as its role in axial skeletogenesis.

MATERIALS & METHODS

Zebrafish maintenance

Zebrafish were bred and maintained at 28.5˚C using an automatic filtration system from Aquatic Eco-Systems Inc, and embryos were staged as previously described [29]. The wild type line used was the Oregon AB* line. The *ewsa/ewsa* line was generated by insertional mutagenesis in a wild-type Ekkwill (EK) background by Znomics Inc, and is maintained as a Maternal Zygotic (MZ) line in our system.

Alizarin red staining

Zebrafish were stained with alizarin red to stain skeletal structures as previously described [30]. Fish were anesthetized with 0.04% Tricaine Methanesulfonate (MS222) and fixed overnight at 4˚C in 4% paraformaldehyde. Pigment was ablated by treatment with 3% H_2O_2 in 1% KOH. Cleared specimens were stained with 0.05% alizarin red dissolved in 1% KOH, destained with successive washes of glycerol/0.25% KOH, and stored in glycerol. Images were taken with a Leica DFC320 camera mounted on a Leica MZ FLIII dissecting microscope.

Immunohistochemistry

Embryos were visualized as previously described [11]. Fixed embryos were permeabilized with methanol at -20˚C overnight, digested with 0.01% trypsin, and then blocked with blocking solution

(5% fetal bovine serum, 0.1% tween-20, in PBS (phosphate buffered saline)). Primary antibodies were applied overnight at 4˚C; embryos were washed thoroughly in wash solution (0.1% tween-20 in PBS); and secondary antibodies were applied overnight at 4˚C. Embryos were then washed thoroughly again. We used a rabbit polyclonal primary antibody (LS-C47340 from LS-Bio) diluted 1:100 and anti-rabbit Alexa 488 diluted 1:250 to visualize Runx2. We used an anti-rabbit polyclonal anti-Collagen X primary antibody (ab58632, abcam) diluted 1:100 and anti-rabbit Alexa 488 diluted 1:250 to visualize Collagen X. We used a solution of WGA (wheat germ agglutinin) Alexa 594 or Alexa 488 diluted 5 µg/mL to visualize cartilage and DAPI diluted 0.5 mg/mL to visualize DNA. Images were taken with an Exi Aqua camera (Q Imaging) mounted on an Eclipse Ti microscope (Nikon).

In situ hybridization

In situ hybridization was performed as previously described (Azuma et al, 2006). Fixed embryos were permeabilized in methanol at -20˚C overnight then washed in PBS. Embryos were then equilibrated in hybridization (HYB) buffer at 60˚C for 3 hours. Embryos were then hybridized overnight at 60˚C with antisense RNA generated with T7 RNA polymerase and DIG-labeled dUTP. Embryos were then treated with anti-DIG antibodies conjugated with alkaline phosphatase (AP) overnight at 4˚C. After equilibration with AP buffer, signal was developed with BM Purple to detect presence of *runx2bP2* mRNA, and then embryos were fixed again in 4% paraformaldehyde at room temperature for 10 minutes. Statistical analysis was performed scoring the embryo as either normal or overexpressed using the Chi-square test with one degree of freedom (*wt/wt*, n=13; MZ *ewsa/ewsa*, n=18).

RESULTS

Runx2 protein expression is upregulated in craniofacial cartilage structures in *MZ ewsa/ewsa mutant* fish 3-6dpf. In Ewing sarcoma, pathogenesis of the disease occurs in bone and soft tissue and as a result of the dominant negative function of EWS/FLI1 over EWS [7]. As a result, understanding the role for Ewing sarcoma protein EWS in the regulation of skeletogenesis is of interest. We have shown previously that Ewsa regulates chondrogenesis through control of chondrogenesis master transcription factor Sox9 and regulates expression of its target genes [12]. The other major transcription factor involved in this process is RUNX2 (Runt-related transcription factor 2), the master transcription factor of skeletogenesis and osteoblastogenesis. During the initial stages of chondrogenesis, SOX9 drives mesenchymal condensations to the chondrocyte lineage and to proliferate [31, 32] and RUNX2 drives chondrocytes to differentiate from prehypertrophy to hypertrophy [16, 17]. We wanted then to understand how expression of Runx2 protein is regulated by Ewsa during zebrafish chondrocyte maturation. In zebrafish, due to a genome duplication event, *runx2* exists as two orthologues, *runx2a* and *runx2b* [33, 34]. Earlier *in situ* hybridization studies have shown that *runx2a* is expressed in zebrafish by the 70% epiboly stage and *runx2b* mRNA is expressed as early as the one-cell stage [33]. Even though both *runx2a* and *runx2b* are detected in early stages, the role of Ewsa in regulation of Runx2 protein expression in later stages during chondrocyte maturation remains unknown. To understand how the dynamics of Runx2 protein expression is regulated by Ewsa during the period of chondrocyte maturation we utilized a commercially available RUNX2 antibody (LSBio LS-C47340). The CBFA1/RUNX2 antibody used in this study was raised in rabbit against a peptide that corresponds to amino acids 262-279 of human RUNX2. BLAST analysis of the immunogen sequence confirms 88% identify with zebrafish Runx2a and Runx2b. Therefore, it is possible the signal seen in embryos using this antibody is both Runx2a and Runx2b. This antibody recognizes the C-terminus of Runx2 to avoid cross-reactivity with the RUNX1 and RUNX3, the other two members of the RUNX gene family which all contain the homologous Runt

DNA-binding domain. Wild-type (*wt/wt*) and MZ *ewsa/ewsa* mutant embryos at 3dpf were subjected to immunohistochemistry using a 1:100 dilution of anti-RUNX2 antibody (Fig. 2). Wild-type embryos at this stage did not express detectable levels of Runx2 protein in the Meckel's cartilage, a structure that undergoes endochondral ossification. At this same stage, MZ *ewsa/ewsa* mutant embryos expressed Runx2 in a greater number of chondrocytes in the Meckel's cartilage compared to wild-type embryos. This trend was also seen in another endochondral cartilage domain, the ceratohyal, at this stage (Fig. 18). To further investigate the dynamics of Runx2 expression in later stages of chondrocyte maturation, wild-type and MZ *ewsa/ewsa* embryos were subject to immunohistochemistry with Runx2 antibody from 4-6dpf. In the MZ *ewsa/ewsa* embryos, the pattern of Runx2 overexpression was continued in the Meckel's cartilages compared to the wild-type (Fig. 3). During these same stages, other craniofacial cartilage domains in MZ *ewsa/ewsa* embryos also displayed an increase of Runx2 expression including the ceratohyal (Fig. 19), palatoquadrate (Fig. 20), hyomandibular (Fig. 21), and ethmoid plate (Fig. 4, Fig. 5). This data suggests that Ewsa plays a role in inhibiting either the transcription of *runx2* or Runx2 translation during these stages of chondrocyte development.

Ewsa does not regulate transcription of *runx2* mRNA in all craniofacial domains. To validate expression of Runx2 protein, *in situ* hybridization using antisense RNA probes specific to *runx2aP2* isoform was performed using 4dpf *wt/wt* and MZ *ewsa/ewsa* embryos (Fig. 6). Expression of *runx2b* has been described previously using *in situ* hybridization [35], and expression of *runx2b* using our probe matches the results described in the literature in the ethmoid plate. Interestingly, over-expression of *runx2bP2* only occurred in the ethmoid plate and not the Meckel's cartilage of MZ *ewsa/ewsa* embryos suggesting a domain-specific regulation of *runx2bP2* transcription by Ewsa. There is no change in expression of *runx2bP2* mRNA transcript in the Meckel's cartilage, ceratohyal, or other craniofacial cartilage domains at this time even though Runx2 protein expression was previously shown to be increased in these domains at 4dpf.

Expression of Collagen X is misregulated in craniofacial structures in MZ *ewsa/ewsa* fish. Ewing sarcoma is a disease characterized as small round blue cells, which is indicative of an undifferentiated phenotype. To further understand how Ewsa plays a role in differentiation of chondrocytes, the differentiation profile of chondrocytes was examined in *wt/wt* and MZ *ewsa/ewsa* fish. The protein expression profile of structural protein collagen, type X, α1 (Col10a1) a late hypertrophic chondrocyte marker, was studied in *wt/wt* and MZ *ewsa/ewsa* fish from at 5dpf. We have also previously shown that expression of Col10a1 protein, a known Runx2 target gene [36], is downregulated in MZ *ewsa/ewsa* fish at 5dpf [12]. These previous data provide further evidence that differentiation of chondrocytes is inhibited at these early stages of development in MZ *ewsa/ewsa* mutants.

Runx2 has been shown to be one of the main drivers of differentiation of prehyperchondrocyte differentiation into hypertrophic chondrocytes and endochondral ossification [17, 37]. Since Runx2 has roles in both chondrocyte and osteoblast differentiation, Runx2 is an attractive target for Ewsa regulation. To understand if Ewsa regulates one of the hypertrophic chondrocyte-specific downstream target genes of Runx2, Collagen X, embryos were subjected to immunohistochemistry from 5dpf using Collagen X antibodies. At 5dpf, MZ *ewsa/ewsa* embryos do not display detectable levels of Collagen X signal in Meckel's cartilage (Fig. 10), as well as another cartilage domain, ceratohyal (Fig. 22). This is indicated by a decrease in signal intensity within these structures compared to *wt/wt*, which shows Collagen X signal within chondrocytes. Interestingly, the hyomandibular cartilage at this stage displays an increase in Collagen X signal at 5dpf (Fig. 23) which may suggest domain-specific regulation of Runx2 transcriptional activity occurs. These data suggest that one of the possible mechanisms by which Ewsa drives chondrocyte differentiation is through regulation of expression of Collagen X, possibly through modulation of Runx2 transcriptional activity.

Mineralization of craniofacial structures is increased in MZ *ewsa/ewsa* mutant fish. We examined if the final stages of skeletogenesis, deposition of mineralized matrix, is regulated by Ewsa. *wt/wt* and MZ *ewsa/ewsa* embryos were subjected to alizarin red staining to detect mineralization in craniofacial domains in 6dpf and 10dpf embryos. At 6dpf, MZ *ewsa/ewsa* embryos show increased intensity of Alizarin red stain compared to *wt/wt* in the parasphenoid (ps) region (Fig. 7). At this stage, mineralization has not yet begun of the endochondral structures, such as Meckel's cartilage and ceratohyal. At 10dpf MZ *ewsa/ewsa* shows greater mineralization in the ps, dentary (d), ceratohyal (ch), and vertebrae (Fig. 8, Table 1). This data matches the results seen in chondrocytes overexpressing Runx2. The dentary, which forms around the Meckel's cartilage, shows an increased expression of mineralization compared to *wt/wt.* The ceratohyal, also displays premature endochondral ossification as does the parasphenoid, a domain near where Runx2 is overexpressed in the ethmoid plate. Premature vertebrae formation, which arise from endochondral ossification, also occurs in MZ *ewsa/ewsa* mutants. A possible explanation for this is that premature overexpression of Runx2 in these domains is inducing premature mineralization. A similar phenotype has been reported in which mice with chondrocyte-specific overexpression of Cbfa1/Runx2 under the control of the type II collagen gene promoter have shown premature chondrocyte maturation and endochondral ossification [38]. This is slightly different than what occurs in our MZ *ewsa/ewsa* fish. Our results suggest that mutants show delayed chondrocyte differentiation in the endochondral structure Meckel's cartilage but show an increase of mineralization in the parasphenoid structure and the dentary, ceratohyal, and vertebrae. There could be several reasons for this difference. First, Runx2 was only overexpressed in cartilage cells in mice whereas in MZ *ewsa/ewsa* fish, there is a loss of Ewsa in the entire organism which may misregulate the function of the osteoblast that deposit mineralized matrix. Also, in mutant fish we have shown an increase of Indian Hedgehog (Ihh) expression in the chondrocytes of the Meckel's cartilage, and Ihh has been shown to prevent chondrocyte

hypertrophy [39]. The overexpression of Ihh may be contributing to delayed differentiation while osteoblast function may be misregulated, leading to premature mineralization.

Notochord cells fail to intercalate and expression of Runx2 is misregulated in the body of MZ *ewsa/ewsa* embryos. Ewing sarcoma development occurs in skeletal elements such as the spine, so we aimed to elucidate the role of Ewsa in axial development. In vertebrates, the notochord gives rise to the nucleus pulposus cells and intervertebral discs in the axial skeleton. MZ *ewsa/ewsa* adult fish show curved spines compared to *wt/wt*. To understand the mechanism behind this phenotype, notochord cells were visualized in live embryos from 5, 6, 8 and 10dpf using brightfield microscopy. The notochord cells of *wt/wt* embryos at 5dpf (data not shown) and at 6dpf intercalate whereas notochord cells of MZ *ewsa/ewsa* mutant zebrafish are more narrow and stacked in a single row (Fig. 11). This trend continued throughout 8dpf and 10dpf (Fig. 24). The cell margins of the notochord cells also appear thicker in MZ *ewsa/ewsa* embryos compared to *wt/wt*. These data suggest that Ewsa plays a critical role in the organization of notochord cells.

We have shown previously that MZ *ewsa/ewsa* mutant zebrafish have curved spines, which may suggest a misregulation of skeletogenesis in this process. We have already seen that Ewsa regulates the expression of Runx2 in craniofacial cartilage, so next we wanted to investigate the possible role of Ewsa-dependent regulation of Runx2 in notochord development. Embryos at 3dpf were subjected to immunohistochemistry using anti-Runx2 antibodies at a 1:100 dilution. At 3dpf, interestingly, Runx2 expression is decreased in the posterior region of the tail inside the notochord of MZ *ewsa/ewsa* mutants compared to *wt/wt* embryos (Fig. 12, Fig. 13). By 5dpf (Fig. 14, Fig. 15) and 6dpf (Fig. 16, Fig. 17) Runx2 protein expression in *wt/wt* embryos extends anteriorly while Runx2 expression in MZ *ewsa/ewsa* mutants remains more posteriorly localized. These data suggest that Ewsa is required for promoting the temporal expression and localization of Runx2 in the notochord. This leads us to speculate that Ewsa's regulation of the localization of Runx2 may also affect the localization and expression of Runx2's downstream target genes, such

as *col10a1,* in these domains. Future study will focus on elucidating how expression of Runx2 target genes are regulated by Ewsa in this domain, since formation of vertebral bodies occurs through an endochondral process, of which Runx2 is an essential component. Col10a1 has already been shown to be expressed premature to vertebral body formation [26] so misregulation of Runx2 expression in these domains may contribute to aberrant Col10a1 expression. Misregulation of this process may lead to aberrant vertebral skeletogenesis and the development of curved spines in MZ *ewsa/ewsa* embryos.

DISCUSSION

Ewsa regulates craniofacial skeletogenesis through regulation of Runx2

To understand the role of Ewsa during skeletogenesis, we investigated the effect of Ewsa on the master regulator of skeletogenesis, Runx2. Our results indicate that Ewsa plays a critical role in controlling expression of Runx2 protein and its target gene *col10a1* and regulating mineralization of craniofacial domains. Together we propose that Ewsa regulates chondrogenesis through regulation of Runx2 expression and transcriptional activity (Fig. 9).

Previous work in this lab has shown that Ewsa plays a critical role in regulating chondrocyte maturation through modulation of the chondrogenesis master transcription factor Sox9 and its transcriptional targets in association with skeletal defects [12]. The other critical transcription factor that drives cartilage differentiation is RUNX2. Tightly regulated control of RUNX2 activity is required to ensure that premature differentiation of chondrocytes and subsequent mineralization does not occur resulting in severe bone defects. This regulation is done partly through SOX9, which has a dominant role on RUNX2 during chondrogenesis [14]. Therefore, controlling the timing of SOX9 and RUNX2 activity is critical for proper cartilage and skeletal development. Since we have shown that EWS directly interacts with SOX9 [12], it is possible that EWS inhibits regulation of RUNX2 through SOX9. Currently, the role of EWS in

RUNX2 regulation has only been described *in vitro* [40]. Elucidating the role of EWS in regulation of RUNX2 *in vivo* is of critical importance.

This report is the first *in vivo* study of EWS-dependent regulation of RUNX2. We first investigated if Runx2 protein levels were affected during chondrocyte differentiation. Here we report that Runx2 protein expression is highly increased in craniofacial chondrocytes of MZ *ewsa/ewsa* fish. These data suggest that Ewsa is essential for controlling the timing of Runx2 protein expression in these domains by inhibiting expression of Runx2. Since *in situ* hybridization only showed an increase of *runx2* mRNA expression in the ethmoid plate domain and not at the Meckel's cartilage or other endochondral structures, these data may suggest that Ewsa does not inhibit Runx2 through transcriptional inhibition in the Meckel's cartilage but through another mechanism. One possible explanation is that Runx2 may be inhibited by Sox9 in these domains. SOX9 has been shown to inhibit RUNX2 function [14] as well as direct it to the lysosome for degradation [15]. It is possible that since Ewsa regulates Sox9 function, Ewsa may be working through Sox9 to inhibit Runx2 protein expression in prehypertrophic chondrocytes to prevent premature differentiation. Previous data in our lab has shown that Sox9a protein is expressed in cartilage structures and this expression is unchanged in both *wt/wt* and MZ *ewsa/ewsa* from 3-6dpf [41], whereas Runx2 is inhibited in *wt/wt* during this period and upregulated in MZ *ewsa/ewsa* mutants. This suggests that Sox9a is unable to inhibit Runx2 expression in these domains in the absence of Ewsa. To understand if Ewsa is required for Sox9-dependent Runx2 inhibition, it will be interesting to study further if loss of Ewsa also contributes to a decrease in lysosomal activity in chondrocytes, since SOX9 directs RUNX2 towards lysosomal degradation. Alternatively, Ewsa may be required to bind to *runx2* mRNA to prevent premature translation [33, 34]. Consistent to the upregulation of Runx2, we also discovered that mineralization of craniofacial structures of MZ *ewsa/ewsa* fish is increased compared to *wt/wt.* These data suggest that Ewsa may work through Sox9 to inhibit Runx2 protein to regulate the timing of mineralization. In the absence of Ewsa, overexpression of Runx2 in cartilage domains may contribute to the phenotype of premature

mineralization, possibly by no longer inhibiting Runx2 expression through Sox9. This is notable because in previous reports, tissue-specific overexpression of Runx2 in mice prehypertrophic chondrocytes led to premature and increased mineralization of long bones and stunted growth [38]. In future studies it will be interesting to identify key signaling molecules in the microenvironment of cartilage structures that may be overexpressed in response to overexpression of Runx2 in chondrocytes, such as Bone morphogenic protein (BMP) and Parathyroid-related peptide (PTHrP). Another possibility is that the premature mineralization phenotype is due to the overexpression of another signaling molecule not directly related to Runx2 overexpression, but another molecule overexpressed due to loss of Ewsa. In MZ *ewsa/ewsa* mutants, we have previously shown that expression of Ctgf is increased in craniofacial domains compared to *wt/wt*. Ctgf is also a known driver for mineralization [42], so Ctgf overexpression may work in parallel with Runx2 overexpression to drive premature mineralization. To test this hypothesis, in future studies we will knock out both *ctgf* and *runx2* in zebrafish chondrocytes and observe whether this loss will rescue the mineralization phenotype.

Ewsa regulates *collagen10a1* expression through modulation of Runx2 transcriptional activity

We discovered that *col10a1* (*colX*) is decreased both at the mRNA and protein level in MZ *ewsa/ewsa* mutant compared to *wt/wt* embryos. The decrease was originally discovered in the Meckel's cartilage. In this study, we further discovered that there are also decreases in *colX* mRNA and protein in other craniofacial domains. Together, these results suggest that Ewsa is required for expression of ColX through regulation of Runx2's transcriptional activity. Runx2 overexpression has been shown to correlate with increased expression of *colX* [38]. Since Runx2 overexpression in MZ *ewsa/ewsa* fish did not correlate with an increase in ColX expression, this suggests that Ewsa is also required for proper Runx2 transcriptional activity. Since ColX is also a marker for hypertrophic chondrocytes, this decrease in expression of ColX indicates that

differentiation of chondrocytes is impaired. For prehypertrophic chondrocytes to differentiate into hypertrophic chondrocytes, expression of *colX* by Runx2 is critical [36]. Since immunohistochemistry analysis only provides information of protein expression and localization, it is still uncertain how Ewsa can specifically be associated with Runx2 to drive transcription of its target genes. Previously, it's been reported that EWS is associated with transcriptional coactivator p300/CBP to regulate transcription and chromatin remodeling [43, 44]. Runx2 has also been shown to interact with p300/CBP to drive expression of its target genes [45]. These reports combined indicate that it is possible that Runx2, EWS, and p300/CBP may form a complex for Runx2 to drive transcription of *colX.* For future studies, it will be interesting to understand if Ewsa forms a complex with p300/CBP and Runx2 to drive target gene expression in chondrocytes. Quantifying gene expression changes using quantitative RT-PCR and RNA-sequencing from cDNA generated using chondrocyte mRNA from *wt/wt* and MZ *ewsa/ewsa* mutants will also provide insight into changes of the transcriptional profile of Runx2 with and without Ewsa. Additionally, in a previous report and data not shown we have demonstrated that Ewsa binds to *ctgf* and *col2a1* loci, and this binding suggests a possible mechanism for transcriptional regulation through chromatin remodeling. It will also be interesting to explore how Ewsa is required in chromatin remodeling for controlling expression of *runx2* and its target gene loci, possibly through recruitment of transcriptional coactivators p300/CBP.

Ewsa is required for proper formation of the notochord and vertebrae formation

In addition to craniofacial structures, we looked at how Ewsa regulates formation of the axial skeleton, because Ewing sarcoma develops in skeletal elements. Previous data from our lab have shown that adult MZ *ewsa/ewsa* fish have curved spines, indicative of defects in the development of their axial skeleton. In zebrafish, a Notch-dependent event occurs that differentiates notochord cells into two distinct cell populations by 16.5 hours post-fertilization (hpf), and at this time the early notochord cells differentiate to form an outer sheath layer and an inner

layer composed of vacuolated cells [22]. The developing notochord depends upon both the rigidity of the extracellular matrix of the notochord sheath as well as the osmotic pressure the vacuolated cells exert on the sheath for structural support [46]. Previous data (not shown) from our lab have shown that Ewsa drives expression of type II collagen in the notochord, and in MZ *ewsa/ewsa* mutants type II collagen expression is upregulated compared to *wt/wt.* We have previously shown via ChIP assay that Ewsa regulates Collagen II expression by interacting with the *col2a1a* locus. Collagen II is a critical component of axial skeleton formation; previous studies utilizing Col2a1-null mice have shown that the notochord persists and IVD formation is inhibited [28]. In this study we found that at 5-6dpf and at 8dpf and 10dpf vacuolated notochord cells display defects in intercalation, evidenced by the single line stacking of vacuolated cells in notochords of MZ *ewsa/ewsa.* One possible explanation for this failure to intercalate is the evidence that increased expression of type II collagen in the sheath may be increasing the rigidity of the ECM. Thus, this rigidity may prevent the vacuolated cells from properly intercalating. Since the notochord cells serve as the foundation for nucleus pulposus cells that later form the IVDs, this phenotype may contribute to the downstream phenotype of adult MZ *ewsa/ewsa* fish displaying curved spines.

As the notochord develops, it undergoes a process very similar to endochondral ossification. The notochord becomes segmented and in regions of vertebrae, expresses type X Collagen, which is eventually replaced by bone, while intervertebral discs are formed from notochord cells [26]. However, the overall development of this process is not well understood. Consistent with results from the cranial skeleton, we discovered that the mineralization of vertebrae occurs prematurely in MZ *ewsa/ewsa* embryos. The result suggests the importance of Ewsa in the mineralization of the axial skeleton. One possible explanation for this result is that overexpression of Runx2 in this region is driving premature mineralization of the axis as well. Since expression of Runx2 target gene *osteocalcin* (*osc*) occurs in the sheath before mineralization [21], overexpression of Runx2 may be contributing to overexpression of Osteocalcin, driving premature mineralization. As a result, it is possible that Ewsa contributes to

mineralization by tightly regulating the formation of both the notochord sheath and expression of genes involved in mineralization. It is currently unknown how the organization of the ECM environment contributes to vertebrae formation. In future studies we will explore how the notochord ECM is misregulated in MZ *ewsa/ewsa* using electron microscopy. A misregulated ECM structure may contribute to the accumulation of several signaling molecules, such as Indian hedgehog (IHH) [47, 48], Bone morphogenic protein (BMP) [48] or other unidentified molecules, contributing to premature mineralization of vertebrae. To test this hypothesis, future work will elucidate the expression profile of these signaling models in the notochord and perform phenocopy experiments either over-expressing or down-regulating expression of signaling molecules contributing to premature vertebral mineralization.

Among the domains in which Runx2 expression is dependent upon Ewsa regulation, it is of utmost importance to identify the exact mechanism behind which Ewsa inhibits Runx2 expression, and how Ewsa regulates the expression of Runx2 target genes, particularly those involved in differentiation such as *col10a1*. Here we provide novel *in vivo* evidence of Ewsa-dependent regulation of Runx2 in endochondral ossification. Since Ewing sarcoma is classified as an undifferentiated small round blue cell tumor, understanding the role of endogenous EWS in differentiate of skeletal tissue, the tissue in which Ewing sarcoma arises, will increase our understanding of the pathogenesis of the disease when EWS function is inhibited. Since RUNX2 is critical for differentiation of chondrocytes, expanding our knowledge of the specific role EWS has on the function and expression of RUNX2 will increase our understanding of the pathogenesis of Ewing sarcoma and skeletogenesis, since defects in differentiation of this tissue type is associated with the disease.

LITERATURE CITED

1. Delattre, O., et al., *Gene fusion with an ETS DNA-binding domain caused by chromosome translocation in human tumours.* Nature, 1992. **359**(6391): p. 162-5.
2. Navarro, D., et al., *The EWS/FLI1 oncogenic protein inhibits expression of the Wnt inhibitor DICKKOPF-1 gene and antagonizes beta-catenin/TCF-mediated transcription.* Carcinogenesis, 2010. **31**(3): p. 394-401.
3. Abaan, O.D., et al., *PTPL1 is a direct transcriptional target of EWS-FLI1 and modulates Ewing's Sarcoma tumorigenesis.* Oncogene, 2005. **24**(16): p. 2715-22.
4. Beauchamp, E., et al., *GLI1 is a direct transcriptional target of EWS-FLI1 oncoprotein.* J Biol Chem, 2009. **284**(14): p. 9074-82.
5. Knoop, L.L. and S.J. Baker, *The splicing factor U1C represses EWS/FLI-mediated transactivation.* J Biol Chem, 2000. **275**(32): p. 24865-71.
6. Knoop, L.L. and S.J. Baker, *EWS/FLI alters 5'-splice site selection.* J Biol Chem, 2001. **276**(25): p. 22317-22.
7. Embree, L.J., M. Azuma, and D.D. Hickstein, *Ewing sarcoma fusion protein EWSR1/FLI1 interacts with EWSR1 leading to mitotic defects in zebrafish embryos and human cell lines.* Cancer Res, 2009. **69**(10): p. 4363-71.
8. Park, H., et al., *Ewing sarcoma EWS protein regulates midzone formation by recruiting Aurora B kinase to the midzone.* Cell Cycle, 2014. **13**(15): p. 2391-9.
9. Li, H., et al., *Ewing sarcoma gene EWS is essential for meiosis and B lymphocyte development.* Journal of Clinical Investigation, 2007. **117**(5): p. 1314-1323.
10. Akiyama, H., et al., *The transcription factor Sox9 has essential roles in successive steps of the chondrocyte differentiation pathway and is required for expression of Sox5 and Sox6.* Genes and Development, 2002. **16**(21): p. 2813-2828.
11. Azuma, M., et al., *Ewing sarcoma protein ewsr1 maintains mitotic integrity and proneural cell survival in the zebrafish embryo.* PloS one, 2007. **2**(10): p. e979 %@ 1932-6203.

12. Merkes, C., et al., *Ewing sarcoma ewsa protein regulates chondrogenesis of Meckel's cartilage through modulation of Sox9 in zebrafish.* PLoS One, 2015. **10**(1): p. e0116627.

13. Yamashita, S., et al., *Sox9 directly promotes Bapx1 gene expression to repress Runx2 in chondrocytes.* Exp Cell Res, 2009. **315**(13): p. 2231-40.

14. Zhou, G., et al., *Dominance of SOX9 function over RUNX2 during skeletogenesis.* Proc Natl Acad Sci U S A, 2006. **103**(50): p. 19004-9.

15. Cheng, A. and P.G. Genever, *SOX9 determines RUNX2 transactivity by directing intracellular degradation.* J Bone Miner Res, 2010. **25**(12): p. 2680-9.

16. Inada, M., et al., *Maturational disturbance of chondrocytes in Cbfa1-deficient mice.* Developmental Dynamics, 1999. **214**(4): p. 279-290.

17. Kim, I.S., et al., *Regulation of chondrocyte differentiation by Cbfa1.* Mech Dev, 1999. **80**(2): p. 159-70.

18. Chen, H., et al., *Runx2 regulates endochondral ossification through control of chondrocyte proliferation and differentiation.* J Bone Miner Res, 2014. **29**(12): p. 2653-65.

19. Komori, T., et al., *Targeted disruption of Cbfa1 results in a complete lack of bone formation owing to maturational arrest of osteoblasts.* Cell, 1997. **89**(5): p. 755-64.

20. Ellis, K., J. Bagwell, and M. Bagnat, *Notochord vacuoles are lysosome-related organelles that function in axis and spine morphogenesis.* J Cell Biol, 2013. **200**(5): p. 667-79.

21. Bensimon-Brito, A., et al., *Distinct patterns of notochord mineralization in zebrafish coincide with the localization of Osteocalcin isoform 1 during early vertebral centra formation.* BMC Developmental Biology, 2012. **12**(1): p. 28.

22. Yamamoto, M., et al., *Mib-Jag1-Notch signalling regulates patterning and structural roles of the notochord by controlling cell-fate decisions.* Development, 2010. **137**(15): p. 2527-37.

23. Stemple, D.L., *Structure and function of the notochord: an essential organ for chordate development.* Development, 2005. **132**(11): p. 2503-12.

24. Sivakamasundari, V. and T. Lufkin, *Bridging the Gap: Understanding Embryonic Interverterbal Disc Development.* Cell & Developmental Biology, 2012. **1**(2): p. 1-15.

25. Smits, P., *Sox5 and Sox6 are required for notochord extracellular matrix sheath formation, notochord cell survival and development of the nucleus pulposus of intervertebral discs.* Development, 2003. **130**(6): p. 1135-1148.

26. Linsenmayer, T.F., E. Gibney, and T.M. Schmid, *Segmental appearance of type X collagen in the developing avian notochord.* Dev Biol, 1986. **113**(2): p. 467-73.

27. Arratia, G., H.P. Schultze, and J. Casciotta, *Vertebral column and associated elements in dipnoans and comparison with other fishes: Development and homology.* Journal of Morphology, 2001. **250**(2): p. 101-172.

28. Aszódi, A., et al., *Collagen II Is Essential for the Removal of the Notochord and the Formation of Intervertebral Discs.* Journal of Cell Biology, 1998. **143**(5): p. 1399-1412.

29. Kimmel, C.B., et al., *Stages of embryonic development of the zebrafish.* Dev Dyn, 1995. **203**(3): p. 253-310.

30. Javidan, Y. and T.F. Schilling, *Development of cartilage and bone.* Methods Cell Biol, 2004. **76**: p. 415-436.

31. Bi, W., et al., *Sox9 is required for cartilage formation.* Nature Genetics, 1999. **22**(1): p. 85-89.

32. Dy, P., et al., *Sox9 directs hypertrophic maturation and blocks osteoblast differentiation of growth plate chondrocytes.* Dev Cell, 2012. **22**(3): p. 597-609.

33. Flores, M.V., et al., *Duplicate zebrafish runx2 orthologues are expressed in developing skeletal elements.* Gene Expr Patterns, 2004. **4**(5): p. 573-81.

34. van der Meulen, T., et al., *Identification and characterisation of two runx2 homologues in zebrafish with different expression patterns.* Biochim Biophys Acta, 2005. **1729**(2): p. 105-17.

35. Flores, M.V., et al., *A hierarchy of Runx transcription factors modulate the onset of chondrogenesis in craniofacial endochondral bones in zebrafish.* Dev Dyn, 2006. **235**(11): p. 3166-76.

36. Zheng, Q., et al., *Type X collagen gene regulation by Runx2 contributes directly to its hypertrophic chondrocyte-specific expression in vivo.* J Cell Biol, 2003. **162**(5): p. 833-42.

37. Ding, M., et al., *Targeting Runx2 expression in hypertrophic chondrocytes impairs endochondral ossification during early skeletal development.* J Cell Physiol, 2012. **227**(10): p. 3446-56.

38. Ueta, C., et al., *Skeletal malformations caused by overexpression of Cbfa1 or its dominant negative form in chondrocytes.* Journal of Cell Biology, 2001. **153**(1): p. 87-99.

39. St-Jacques, B., M. Hammerschmidt, and A.P. McMahon, *Indian hedgehog signaling regulates proliferation and differentiation of chondrocytes and is essential for bone formation.* Genes & Development, 1999. **13**(16): p. 2072-2086.

40. Li, X., et al., *The Ewing's sarcoma fusion protein, EWS-FLI, binds Runx2 and blocks osteoblast differentiation.* J Cell Biochem, 2010. **111**(4): p. 933-43.

41. Lewin, S.J., *The role of Ewing's sarcoma protein EWS in endochondral ossification and angiogenesis*, in *Molecular Biosciences*. 2015, University of Kansas: ProQuest LLC. p. 47.

42. Safadi, F.F., et al., *Expression of connective tissue growth factor in bone: its role in osteoblast proliferation and differentiation in vitro and bone formation in vivo.* J Cell Physiol, 2003. **196**(1): p. 51-62.

43. Araya, N., et al., *Cooperative interaction of EWS with CREB-binding protein selectively activates hepatocyte nuclear factor 4-mediated transcription.* J Biol Chem, 2003. **278**(7): p. 5427-32.

44. Rossow, K.L. and R. Janknecht, *The Ewing's sarcoma gene product functions as a transcriptional activator.* Cancer research, 2001. **61**(6): p. 2690-5.

45. Sierra, J., et al., *Regulation of the Bone-Specific Osteocalcin Gene by p300 Requires Runx2/Cbfa1 and the Vitamin D3 Receptor but Not p300 Intrinsic Histone Acetyltransferase Activity.* Molecular and Cellular Biology, 2003. **23**(9): p. 3339-3351.

46. Adams, D.S., R. Keller, and M.A. Koehl, *The mechanics of notochord elongation, straightening and stiffening in the embryo of Xenopus laevis.* Development, 1990. **110**(1): p. 115-30.

47. DiPaola, C.P., et al., *Molecular signaling in intervertebral disk development.* Journal of Orthopaedic Research, 2005. **23**(5): p. 1112-1119.

48. Watanabe, Y., et al., *Two domains in vertebral development: antagonistic regulation by SHH and BMP4 proteins.* Development, 1998. **2639**(125): p. 2631-2639.

FIGURES

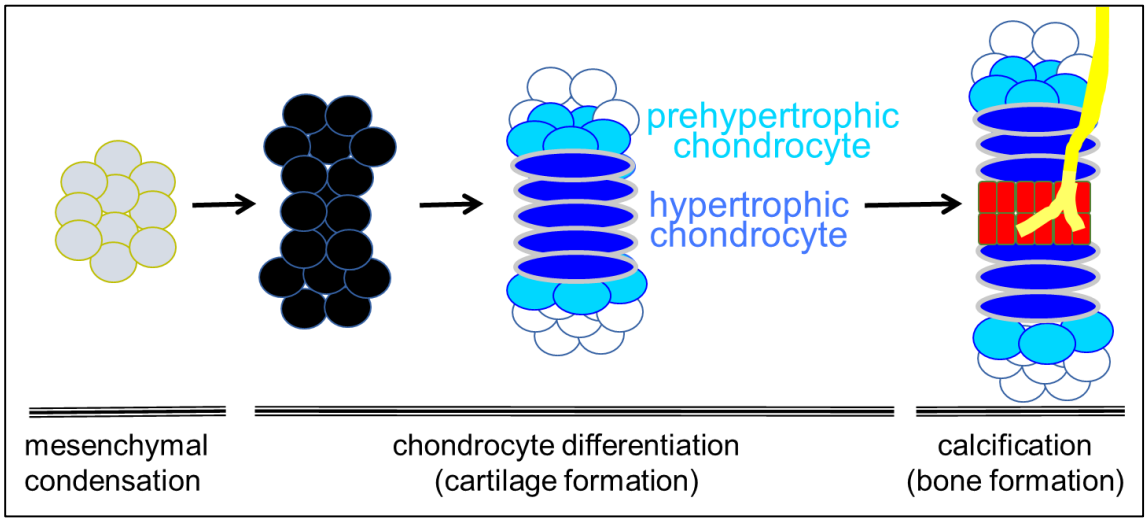

Figure 1. Endochondral ossification. Endochondral ossification is the developmental process of the formation of long bones that relies on a cartilaginous intermediate. Mesenchymal precursors differentiate into proliferating chondrocytes, which then differentiate into prehypertrophic chondrocytes and later hypertrophic chondrocytes. Hypertrophic chondrocytes then construct ECM and die and become invaded by blood vessels that deposit osteoblasts, which then deposit bone on the remaining ECM.

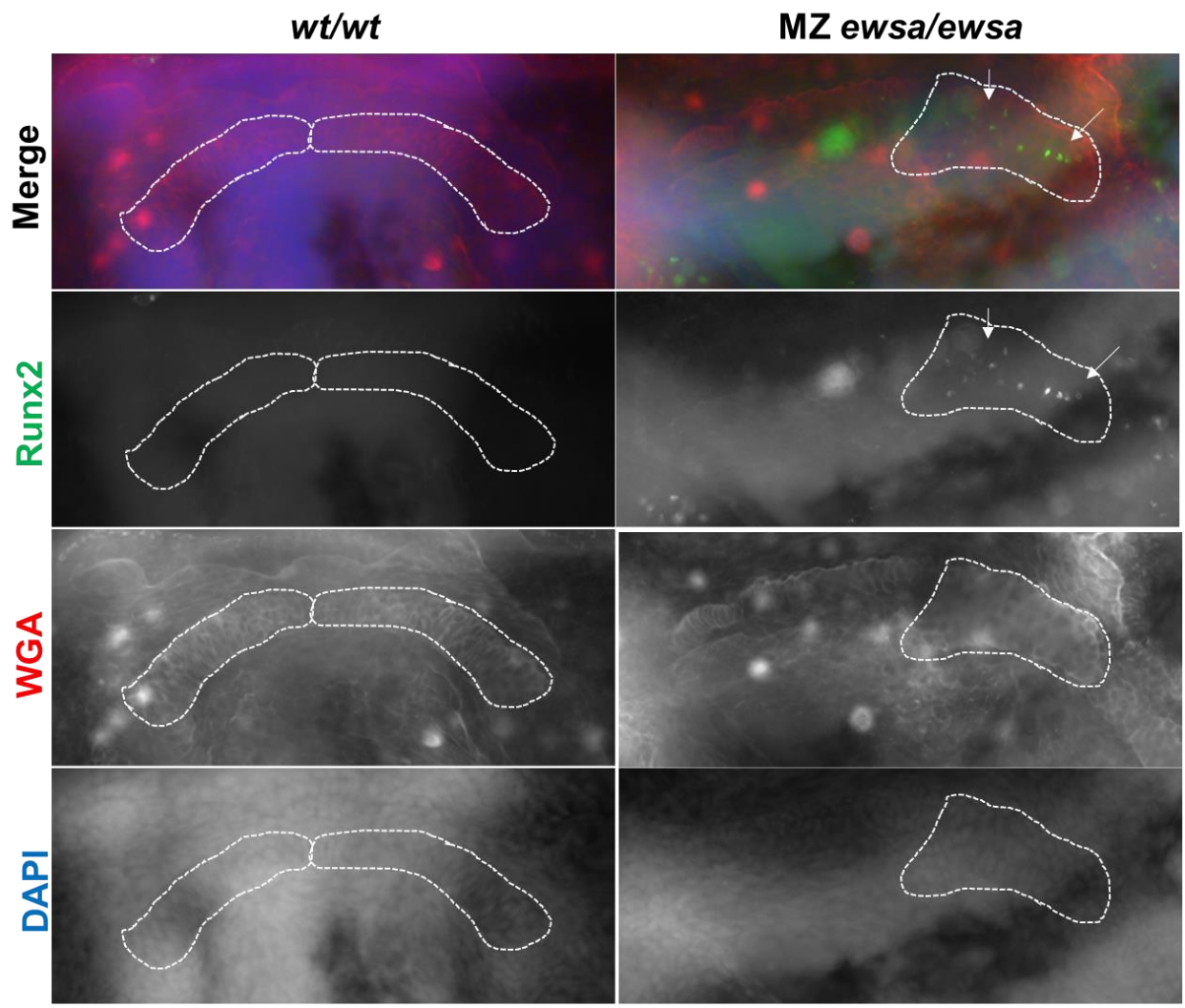

Figure 2. Runx2 is expressed in Meckel's cartilage of 3dpf MZ *ewsa/ewsa* embryos but not *wt/wt*. Immunohistochemistry of wild-type (*wt/wt*) and maternal zygotic (MZ) *ewsa/ewsa* Meckel's cartilage at 3dpf with RUNX2 antibody. Runx2 protein is not expressed at detectable levels in *wt/wt* embryos but is expressed in a higher number of chondrocytes in MZ *ewsa/ewsa* mutants at 3dpf. Antibody dilution 1:100. *wt/wt* n=8; MZ *ewsa/ewsa* n=10 ($p<0.001$, Chi-square test with one degree of freedom).

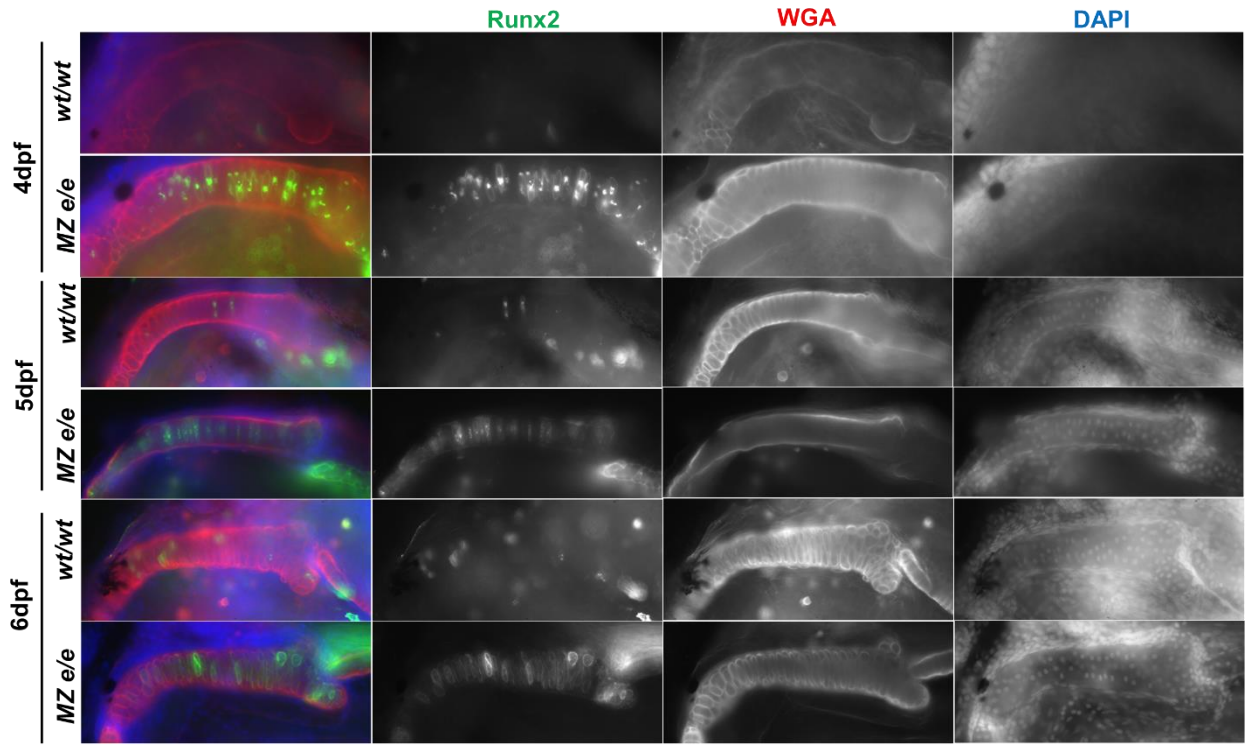

Figure 3: Runx2 expression in wild-type and MZ *ewsa/ewsa* Meckel's cartilage from 4-6dpf. Immunohistochemistry of wild-type (*wt/wt*) and maternal zygotic (MZ) *ewsa/ewsa* mutant embryos with RUNX2 antibody shows that expression of Runx2 protein is present in the Meckel's cartilage at 4-6dpf. Structures were scored as either 'overexpression' or 'low expression' of Runx2. At 4dpf, 2/27 (7%) *wt/wt* embryos (n=27) display overexpression and 40/41 (98%) of MZ *ewsa/ewsa* zebrafish display overexpression of Runx2 ($p<0.005$). At 5dpf, 1/10 (10%) *wt/wt* embryos showed strong expression and 11/11 (100%) MZ *ewsa/ewsa* embryos showed high expression of Runx2 ($p<0.001$). At 6dpf 0/8 (0%) *wt/wt* embryos (n=8) display overexpression and 8/8 (100%) of MZ *ewsa/ewsa* embryos (n=8) display overexpression. Statistical analysis performed using Chi-square test with one degree of freedom. Antibody dilution 1:100.

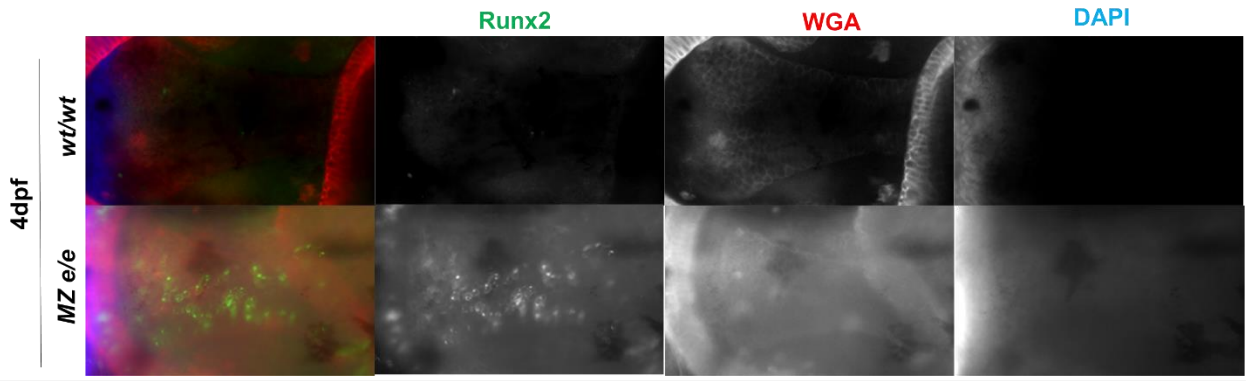

Figure 4. **Runx2 expression in wild-type and MZ *ewsa/ewsa* craniofacial cartilage from 4dpf.** Immunohistochemistry of wild-type (*wt/wt*) and maternal zygotic (MZ) *ewsa/ewsa* mutant embryos with RUNX2 antibody shows that expression of Runx2 protein is present in a higher number of chondrocytes of ethmoid plate at 4pf in MZ *ewsa/ewsa* zebrafish compared to *wt/wt* embryos. Antibody dilution 1:100.

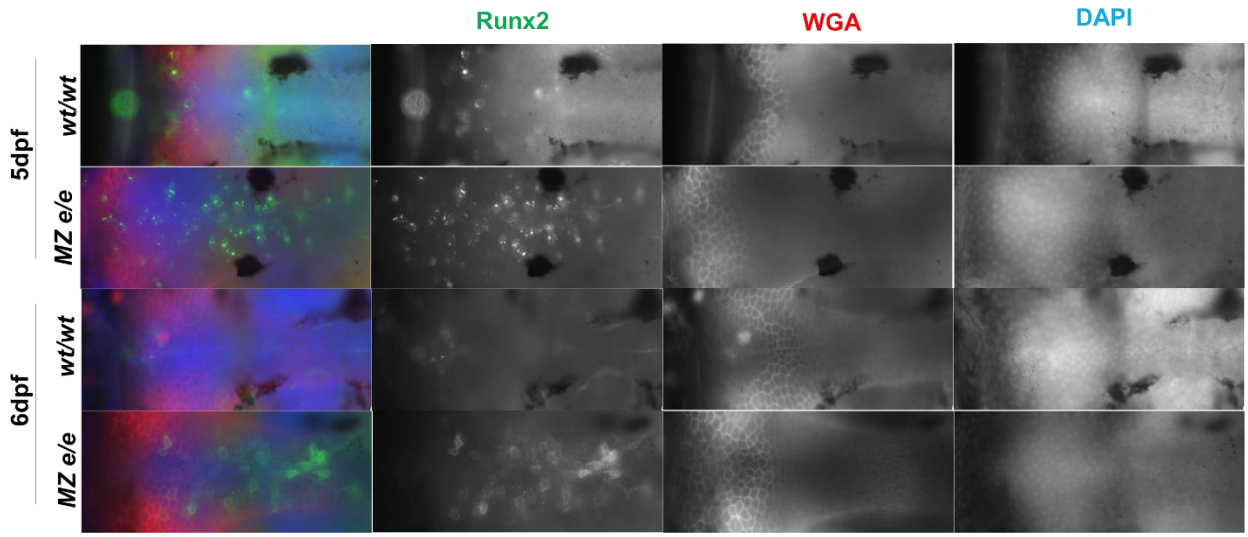

Figure 5: Runx2 expression in wild-type and MZ *ewsa/ewsa* ethmoid plate from 5dpf. Immunohistochemistry of wild-type (*wt/wt*) and maternal zygotic (MZ) *ewsa/ewsa* mutant embryos with RUNX2 antibody shows that expression of Runx2 protein is present in a higher number of chondrocytes of the ethmoid plate at 5-6dpf in MZ *ewsa/ewsa* zebrafish compared to *wt/wt* embryos. Antibody dilution 1:100.

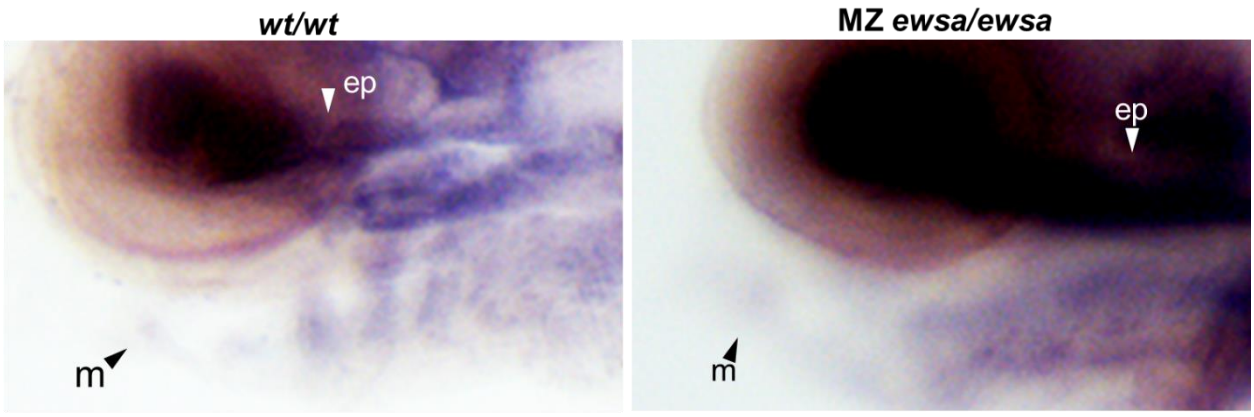

Figure 6. Expression of *runx2bP2* transcripts increased in MZ *ewsa/ewsa* mutants. In situ hybridization using an anti-sense *runx2bP2* isoform probe shows increased expression in the ep region but not in Meckel's cartilage. *wt/wt* n=13; MZ *ewsa/ewsa*, n=18. 56% (10/18) MZ *ewsa/ewsa* embryos showed increased expression in ep compared to *wt/wt* ($p<0.001$, Chi-square test with one degree of freedom). Abbreviations: ep=ethmoid plate; m=Meckel's cartilage.

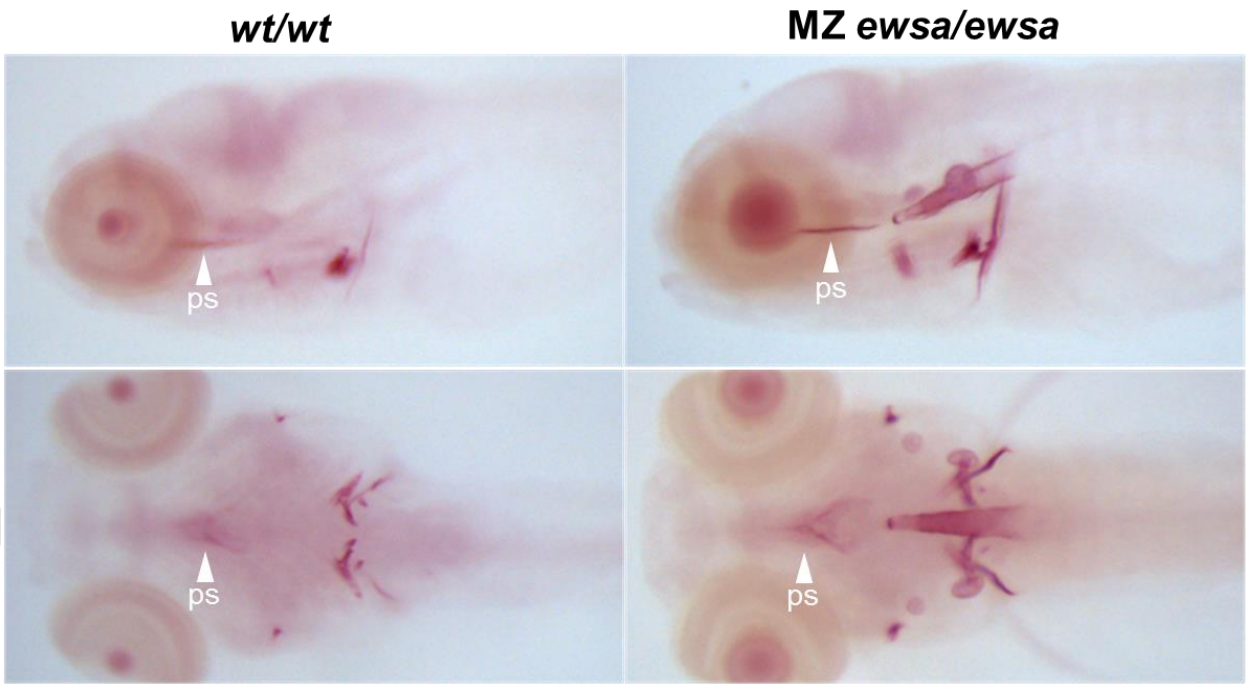

Figure 7. Mineralization is increased in MZ *ewsa/ewsa* embryos compared to *wt/wt* at 6dpf. Alizarin red staining shows an increase of mineralization in the MZ *ewsa/ewsa* embryos. Embryos were scored as having either a high or low amount of mineralization indicated by more intense signal and extended anteriorly. 0/8 (0%) of *wt/wt* embryos (n=8) displayed high mineralization and 9/9 (100%) MZ *ewsa/ewsa* embryos (n=9) displayed high degrees of mineralization ($p<0.001$). Statistical analysis performed using Chi-square test with one degree of freedom. Abbreviation: ps, parasphenoid.

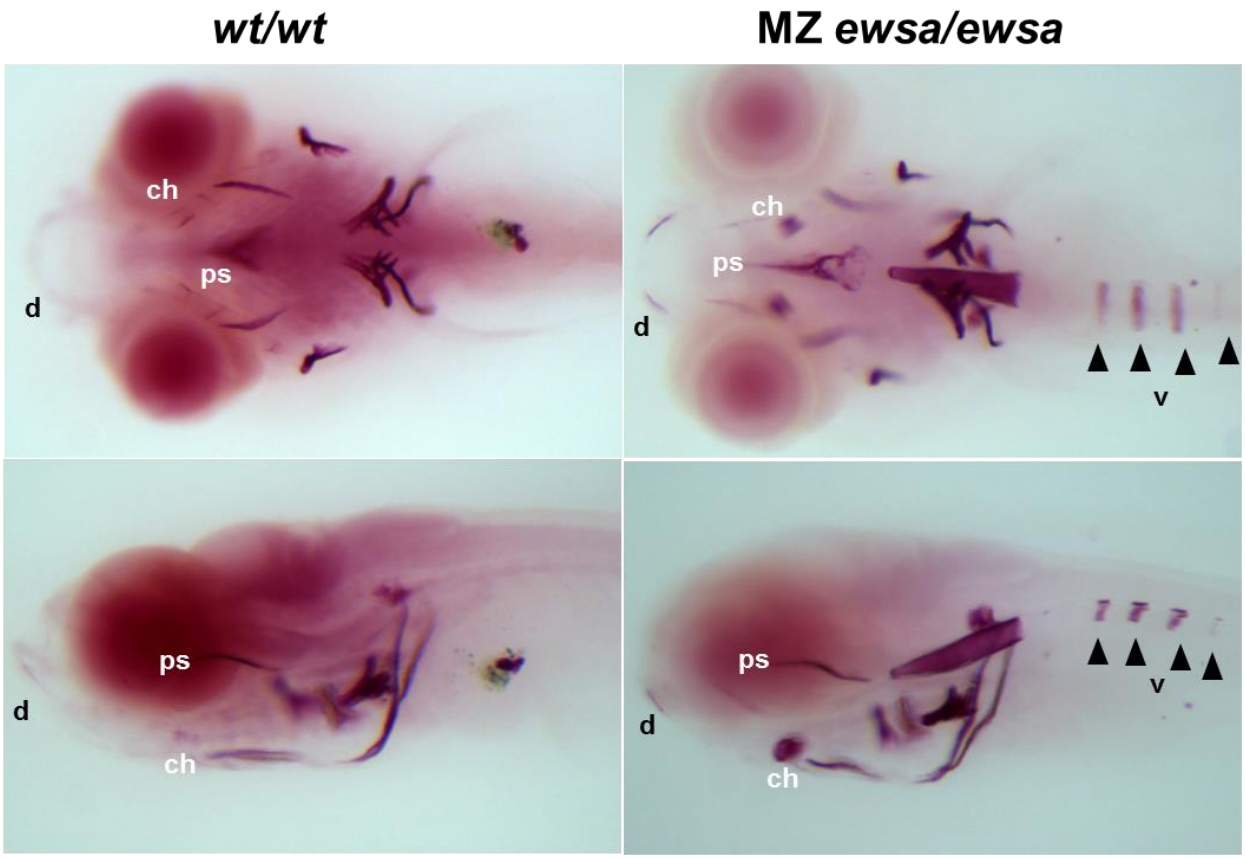

Figure 8. Mineralization is increased in MZ *ewsa/ewsa* embryos compared to *wt/wt* at 10dpf. Alizarin red staining shows an increase of mineralization in the MZ *ewsa/ewsa* embryos. *wt/wt*, n=8; MZ *ewsa/ewsa*, n=9. 4/9 MZ *ewsa/ewsa* displayed vertebrae. Abbreviations: ps, parasphenoid; ch, ceratohyal; d, dentary. Black triangles indicate vertebrae.

Table 1: % of craniofacial structures displaying high mineralization at 10dpf					
	d	ps	ch	v	n=
wt/wt	0/8 (0%)	0/8 (0%)	0/8 (0%)	0/8 (0%)	8
MZ *ewsa/ewsa*	9/9 (100%)*	9/9 (100%)*	9/9 (100%)*	9/9 (100%)**	9

*p<0.001, **p<0.05

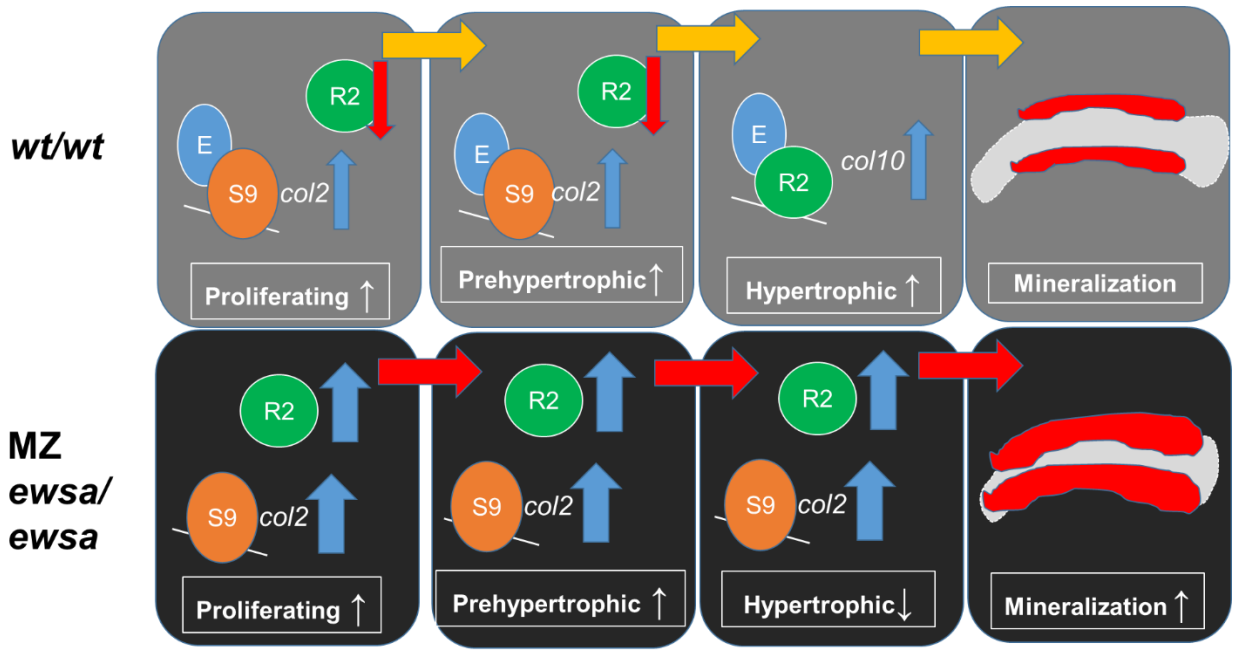

Figure 9. Model of Ewsa-Runx2 modulation in skeletogenesis. In early proliferating and prehypertrophic chondrocytes, Sox9 is the dominant transcription factor, and heterodimerizes with Ewsa to regulate transcription of its target genes. In these early chondrocytes, Sox9 has a dominant negative function on Runx2 and directs its degradation toward the lysozome. Sox9 protein expression levels are the same from 3-6dpf in both *wt/wt* and MZ *ewsa/ewsa* (data not shown). In *wt/wt*, this corresponds with a decrease in Runx2 expression at this time. In MZ *ewsa/ewsa* chondrocytes Runx2 expression remains increased, suggesting that Sox9 depends on Ewsa to direct Runx2 degradation.

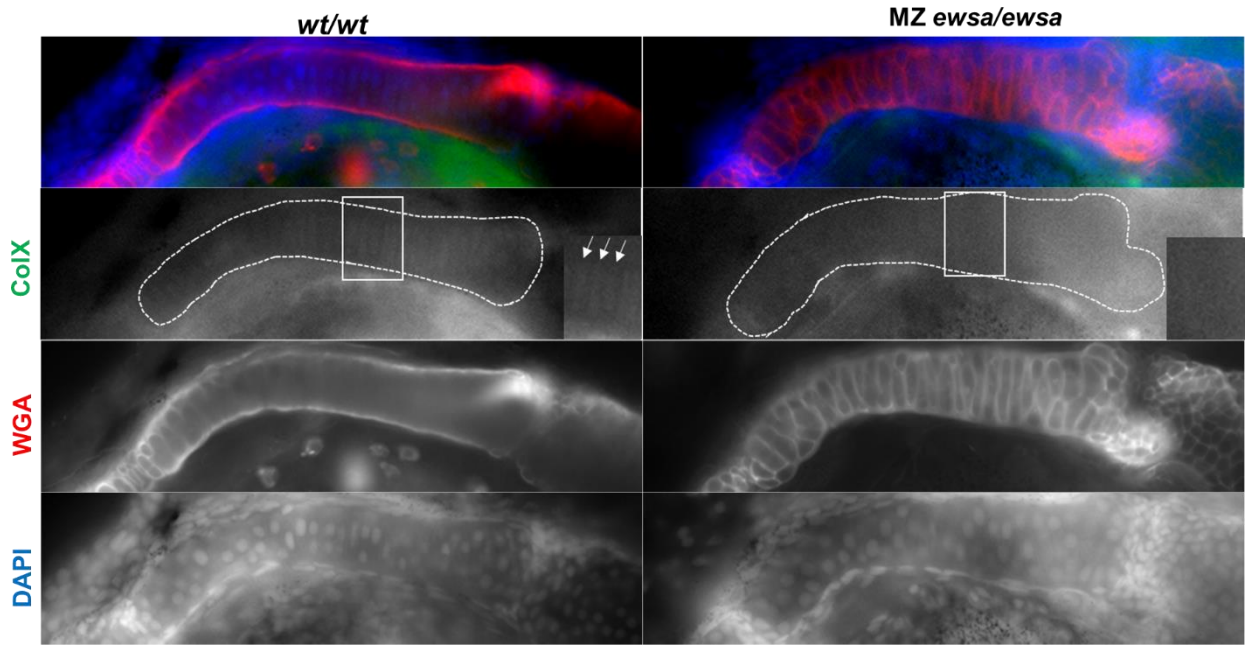

Figure 10. Collagen10a1 expression is decreased in Meckel's cartilage of MZ *ewsa/ewsa* mutant embryos compared to *wt/wt* at 5dpf. Ventral views of Meckel's cartilage of 5dpf *wt/wt* and MZ *ewsa/ewsa* mutant embryos (anterior to left) visualized by immunohistochemistry using anti-Collagen10a1 antibodies (green) and cartilage stain WGA (red). Meckel's cartilages were scored as either 'expressing' ColX or 'not expressing' ColX.

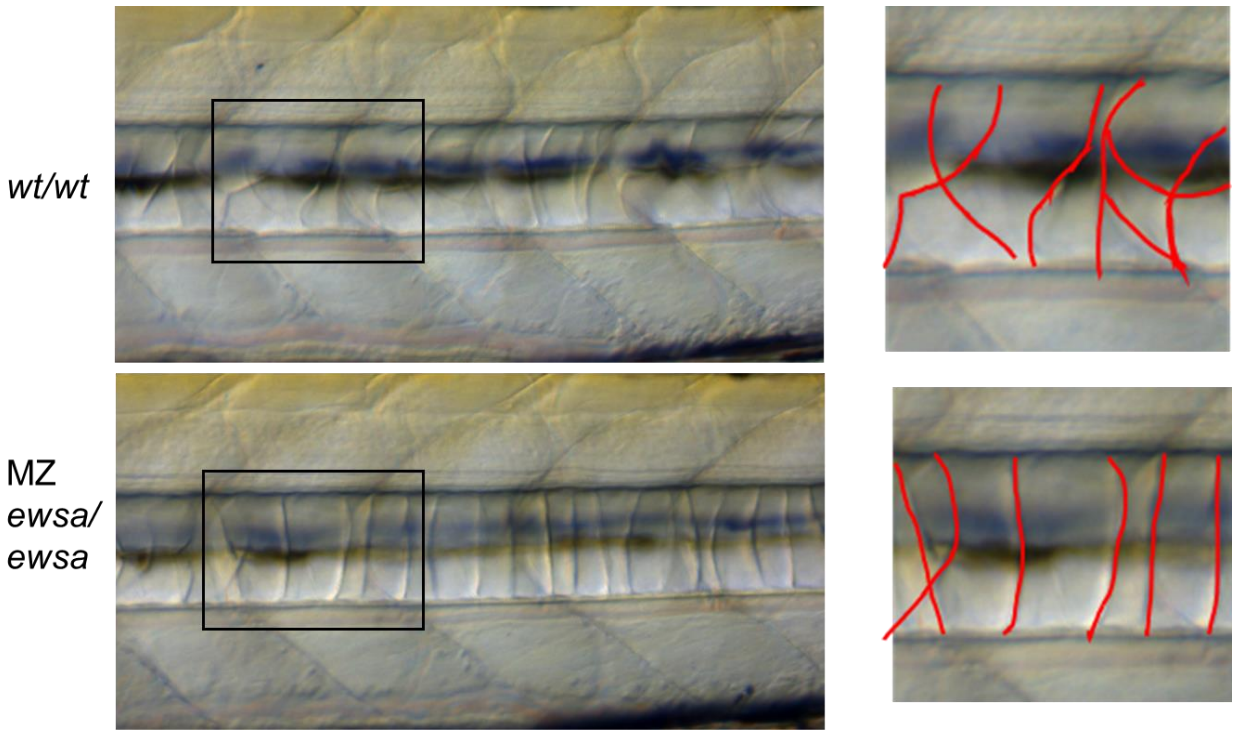

Figure 11. Notochord cells fail to intercalate in MZ *ewsa/ewsa* mutants compared to *wt/wt.* Brightfield analysis of the notochord cells of 6dpf embryos. MZ *ewsa/ewsa* mutants show thicker notochord boundaries and fewer intercalated cells. Magnification 200x. 0% of *wt/wt* (n=5) nc cells failed to intercalate. 100% MZ e*wsa/ewsa* (n=5) nc cells failed to intercalate.

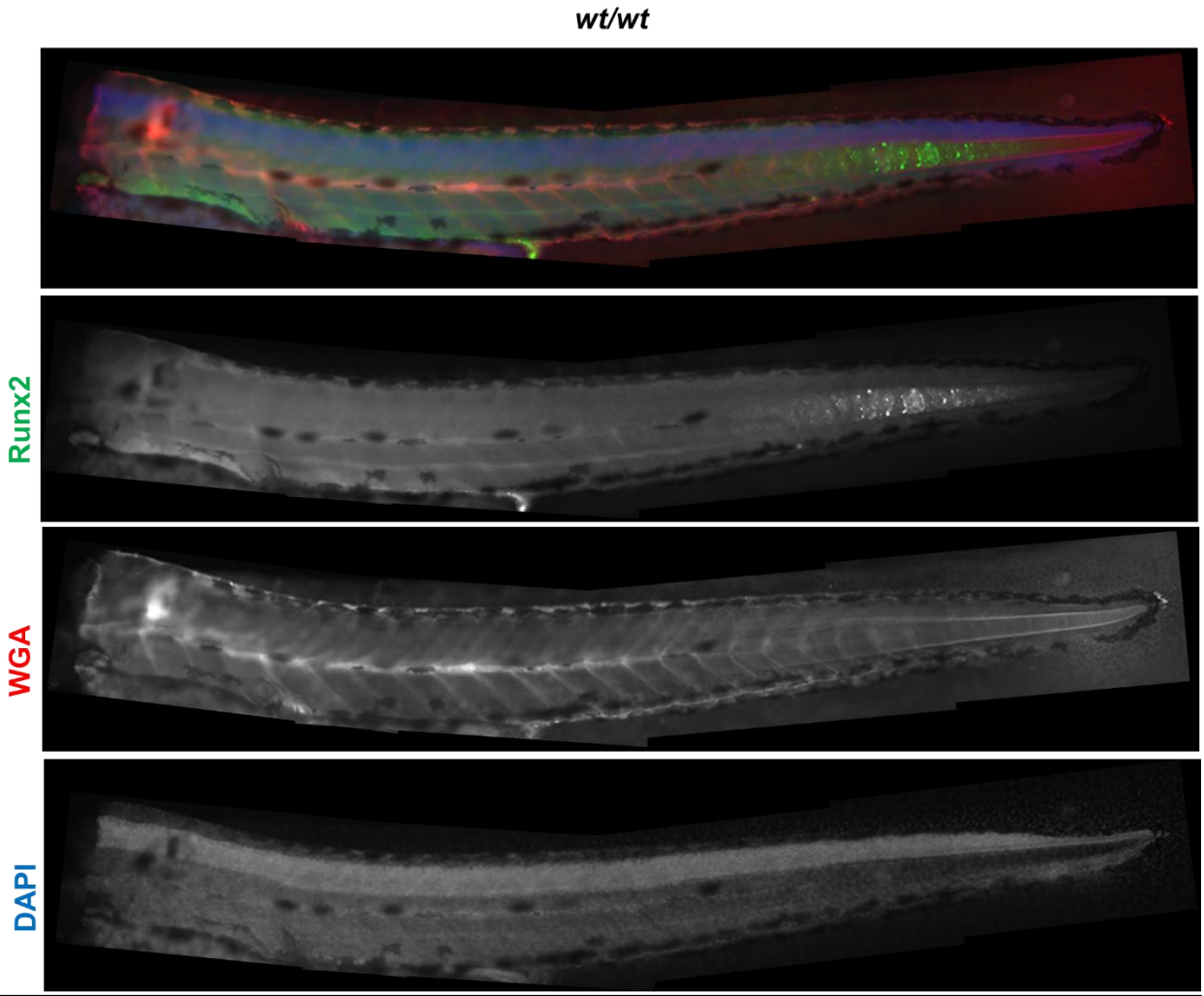

Figure 12. Runx is expressed in the posterior tail at 3dpf. Runx2 is expressed inside the notochord in the posterior portion of the tail. Posterior to right, ventral below. Antibody concentration 1:100.

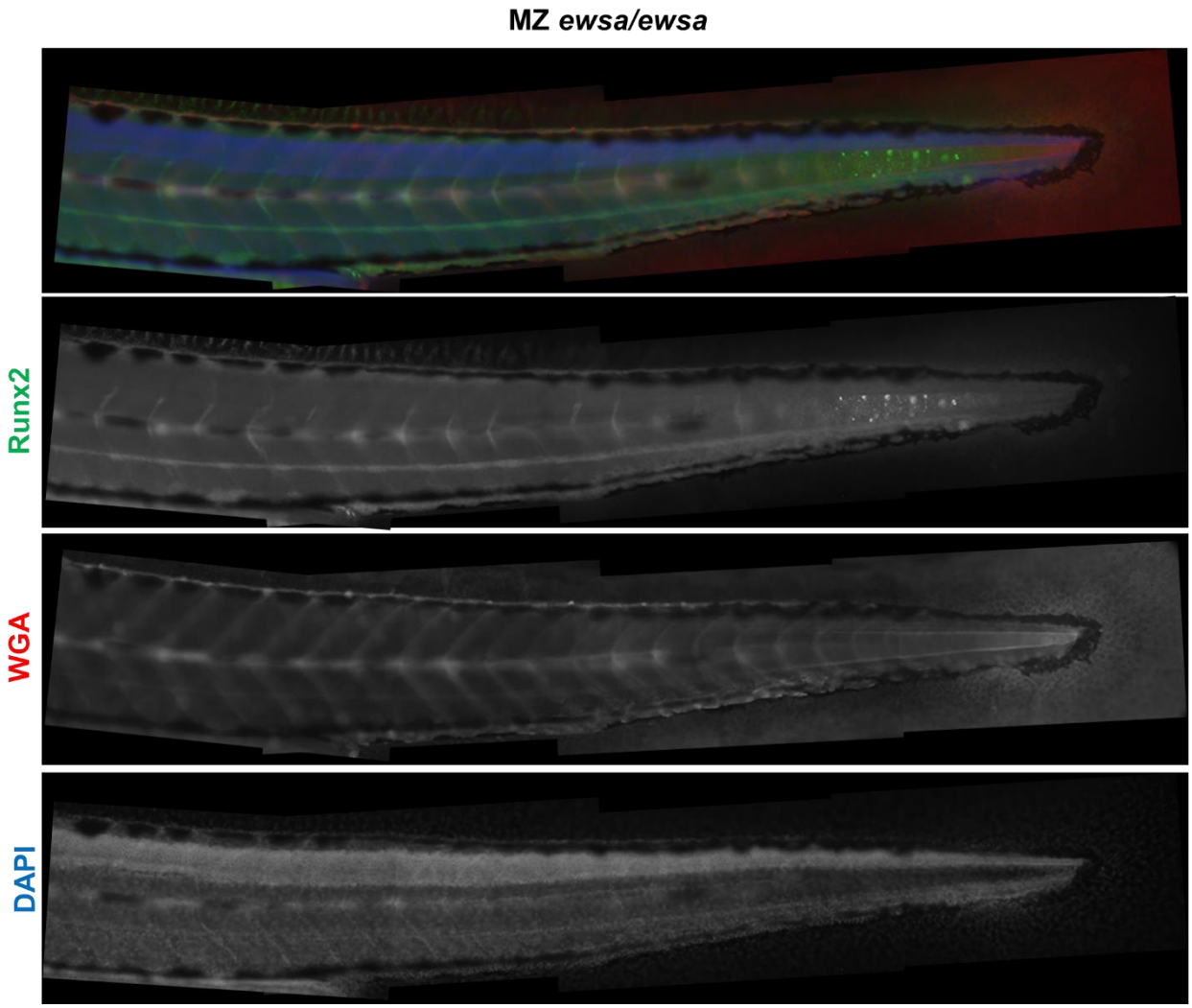

Figure 13. Runx2 expression is decreased in the posterior tail of 3dpf MZ *ewsa/ewsa* mutants compared to *wt/wt.* Runx2 is expressed inside the notochord in the posterior portion of the tail in MZ *ewsa/ewsa* mutants, but at a decreased intensity compared to *wt/wt*. Posterior to right, ventral below. Antibody concentration 1:100.

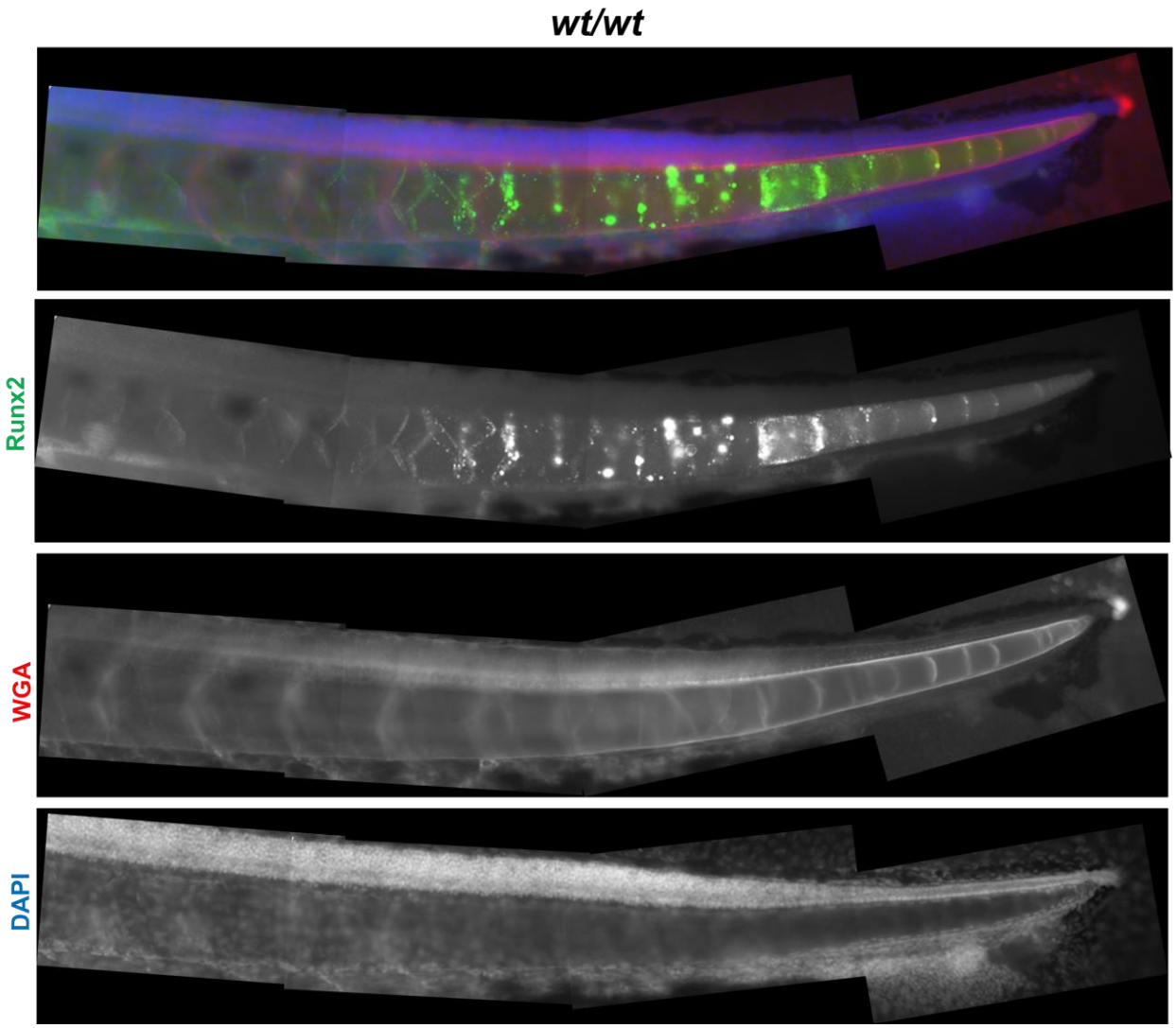

Figure 14. Runx2 expression extends more anterior at 5dpf. Runx2 is expressed inside the notochord in the posterior portion of the tail and expression begins extending anteriorly at 5dpf. Posterior to right, ventral below. Antibody concentration 1:100.

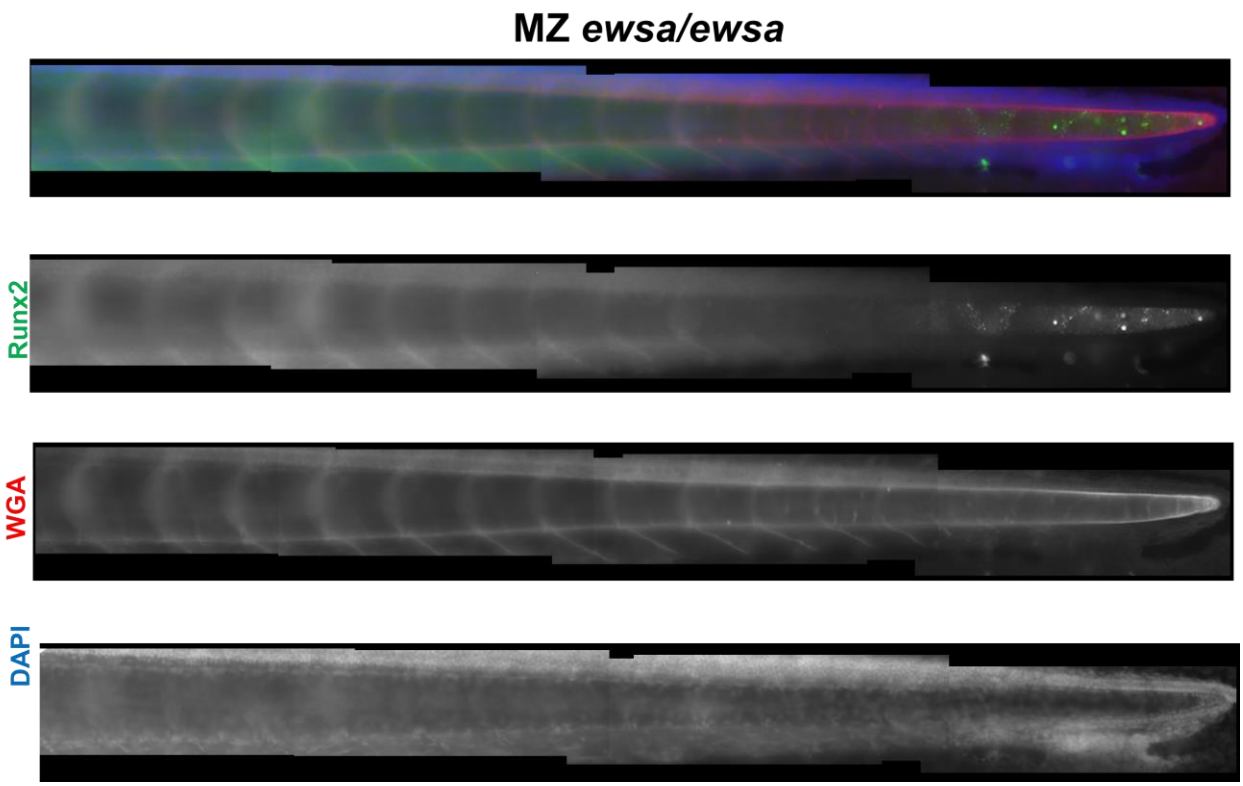

Figure 15. Runx2 expression in the MZ *ewsa/ewsa* mutants remains decreased in the posterior portion of the tail by 5pdf compared to *wt/wt*. Runx2 is expressed inside the notochord in the posterior portion of the tail and expression remains decreased compared to *wt/wt* 5dpf. Posterior to right, ventral below. Antibody concentration 1:100.

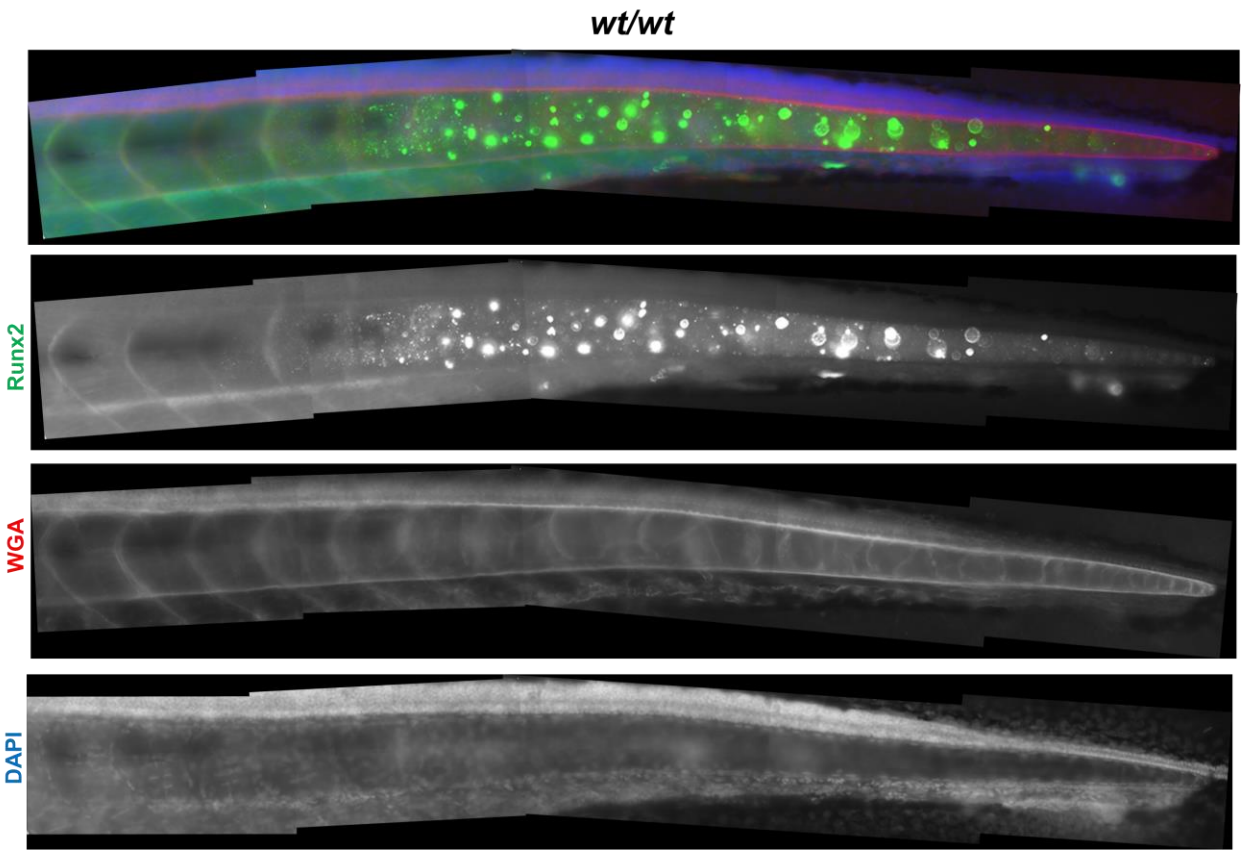

Figure 16. Runx2 expression extends more anterior at 6dpf. Runx2 is expressed inside the notochord in the posterior portion of the tail and expression continues extending anteriorly at 6dpf. Posterior to right, ventral below. Antibody concentration 1:100.

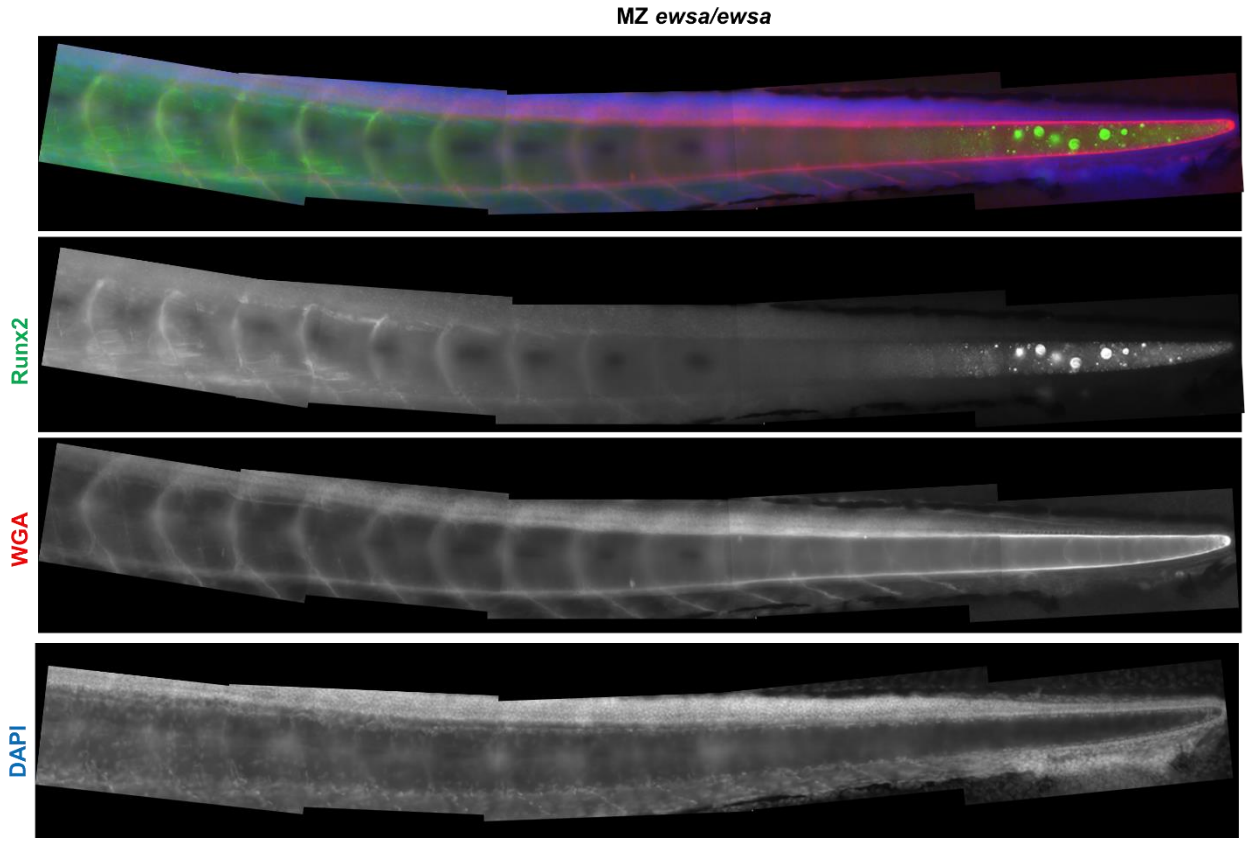

Figure 17. Runx2 expression extends more anterior at 6dpf. Runx2 is expressed inside the notochord in the posterior portion of the tail and expression begins extending anteriorly at 6dpf, but expression is decreased compared to *wt/wt*. Posterior to right, ventral below. Antibody concentration 1:100.

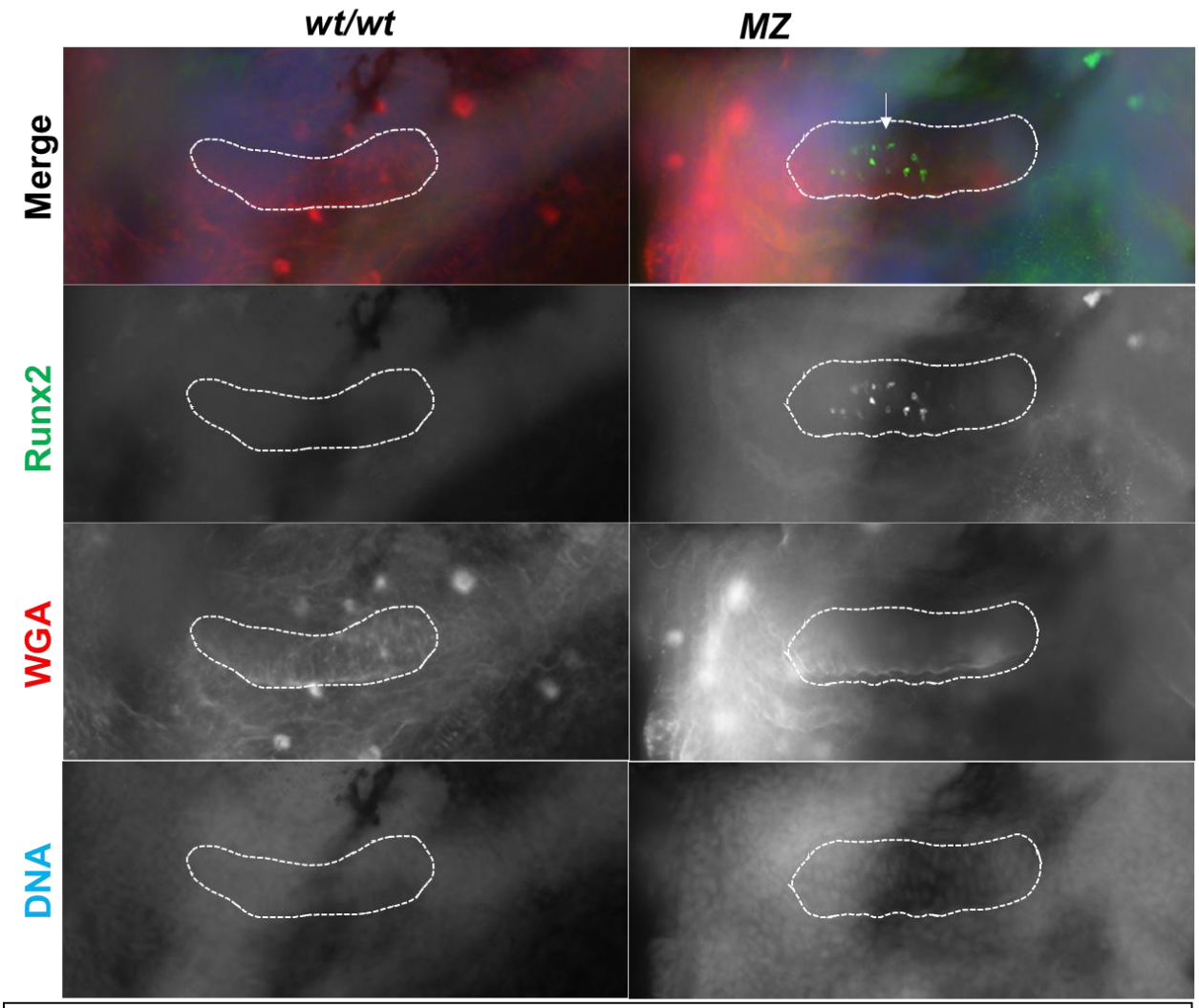

Figure 18. Runx2 is expressed in ceratohyal cartilage of 3dpf MZ *ewsa/ewsa* embryos but not *wt/wt*. Immunohistochemistry of wild-type (*wt/wt*) and maternal zygotic (MZ) *ewsa/ewsa* ceratohyal cartilage at 3dpf with RUNX2 antibody. Runx2 protein is not expressed at detectable levels in *wt/wt* embryos but is expressed in a higher number of chondrocytes in MZ *ewsa/ewsa* mutants at 3dpf. Antibody dilution 1:100.

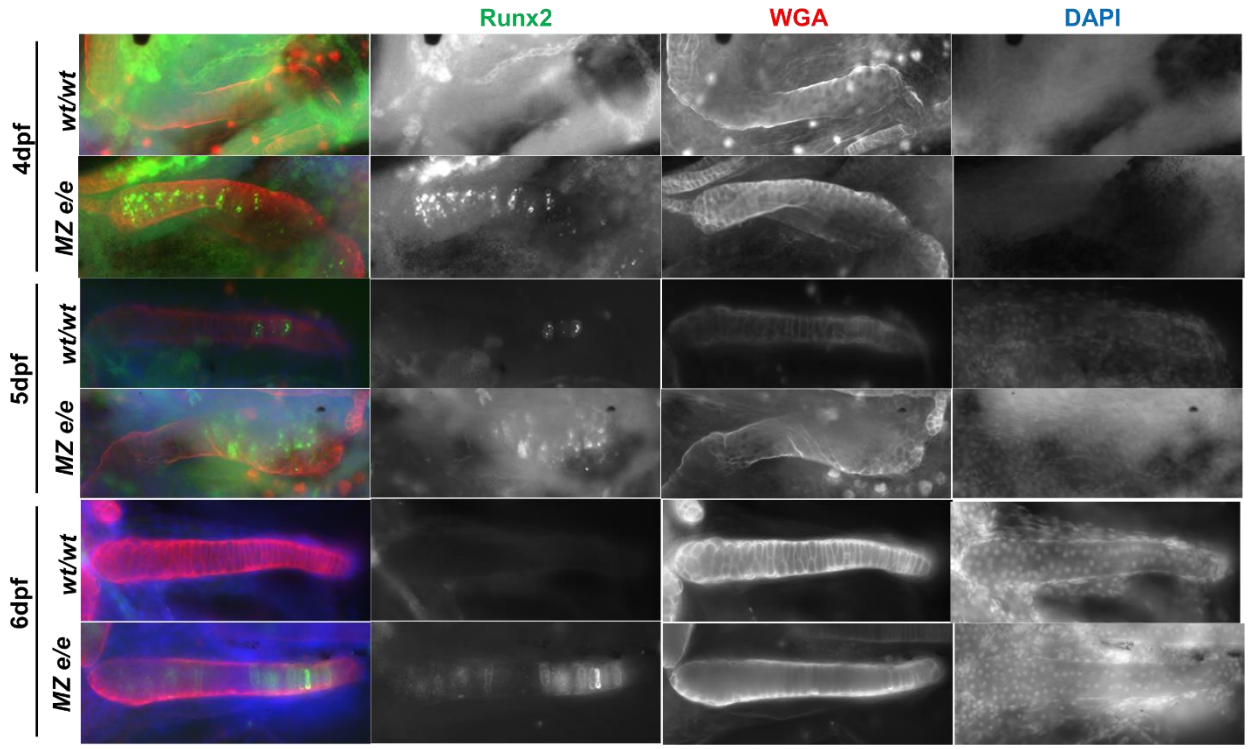

Figure 19: Runx2 expression in wild-type and MZ *ewsa/ewsa* ceratohyal from 4-6dpf. Immunohistochemistry of wild-type (*wt/wt*) and maternal zygotic (MZ) *ewsa/ewsa* mutant embryos with RUNX2 antibody shows that expression of Runx2 protein is present in the ceratohyal of 4dpf MZ *ewsa/ewsa* zebrafish but not *wt/wt* embryos. Expression of Runx2 persists through 6dpf, with a greater number of chondrocytes expressing Runx2 in MZ *ewsa/ewsa* compared to *wt/wt* embryos at all stages. Antibody dilution 1:100.

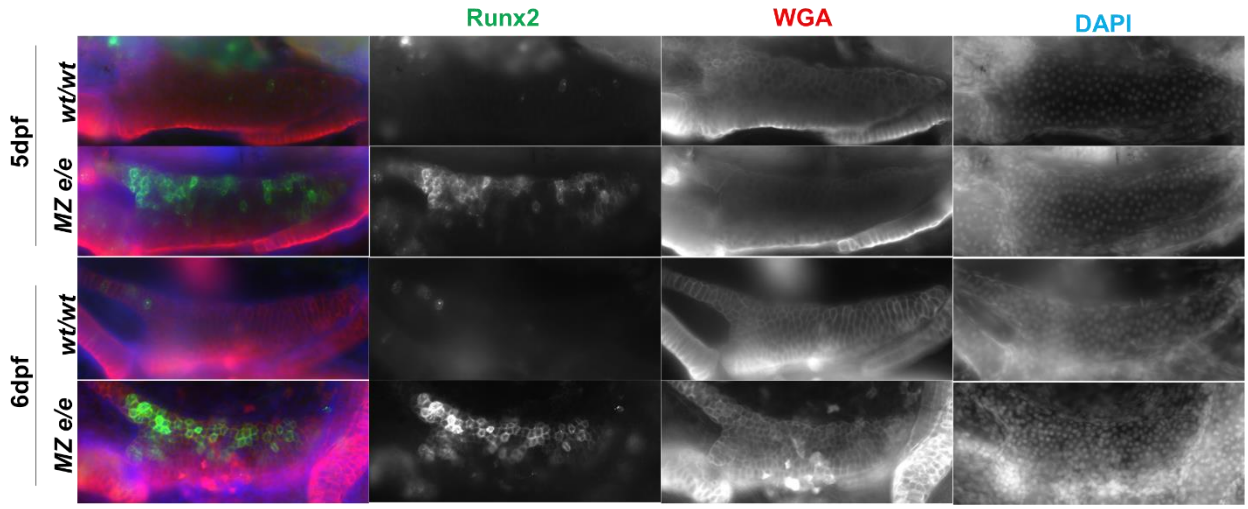

Figure 20: Runx2 expression in wild-type and MZ *ewsa/ewsa* craniofacial cartilage from 5-6dpf. Immunohistochemistry of wild-type (*wt/wt*) and maternal zygotic (MZ) *ewsa/ewsa* mutant embryos with RUNX2 antibody shows that expression of Runx2 protein is present in a higher number of chondrocytes of the palatoquadrate cartilage at 5-6dpf in MZ *ewsa/ewsa* zebrafish compared to *wt/wt* embryos. Antibody dilution 1:100.

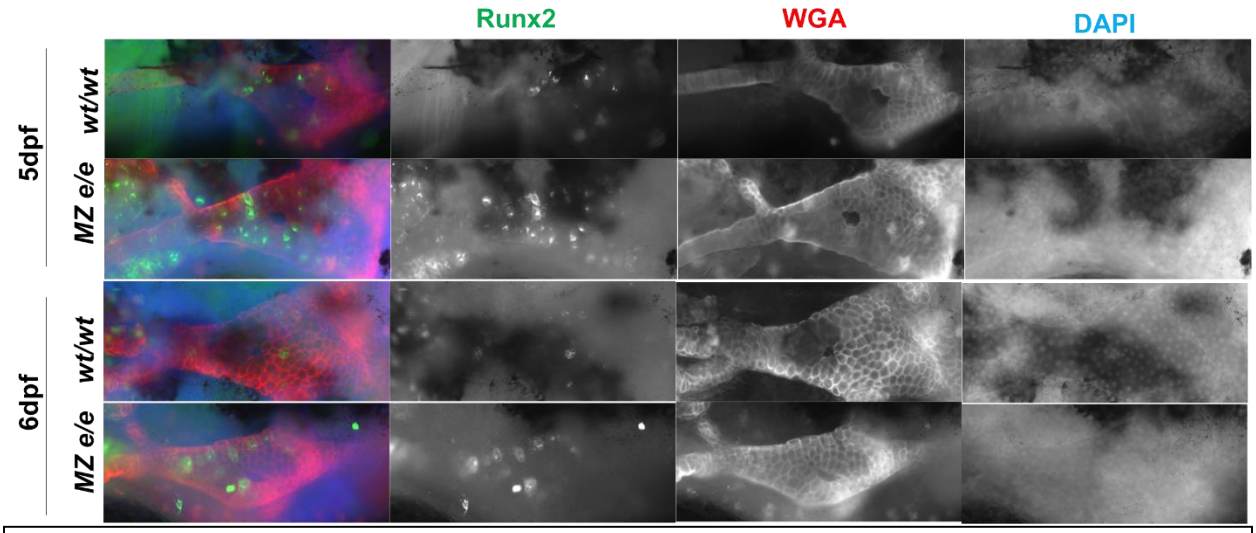

Figure 21: Runx2 expression in wild-type and MZ *ewsa/ewsa* craniofacial cartilage from 5dpf. Immunohistochemistry of wild-type (*wt/wt*) and maternal zygotic (MZ) *ewsa/ewsa* mutant embryos with RUNX2 antibody shows that expression of Runx2 protein is present in a higher number of chondrocytes of the hyomandibular cartilage at 5-6dpf in MZ *ewsa/ewsa* zebrafish compared to *wt/wt* embryos. Antibody dilution 1:100.

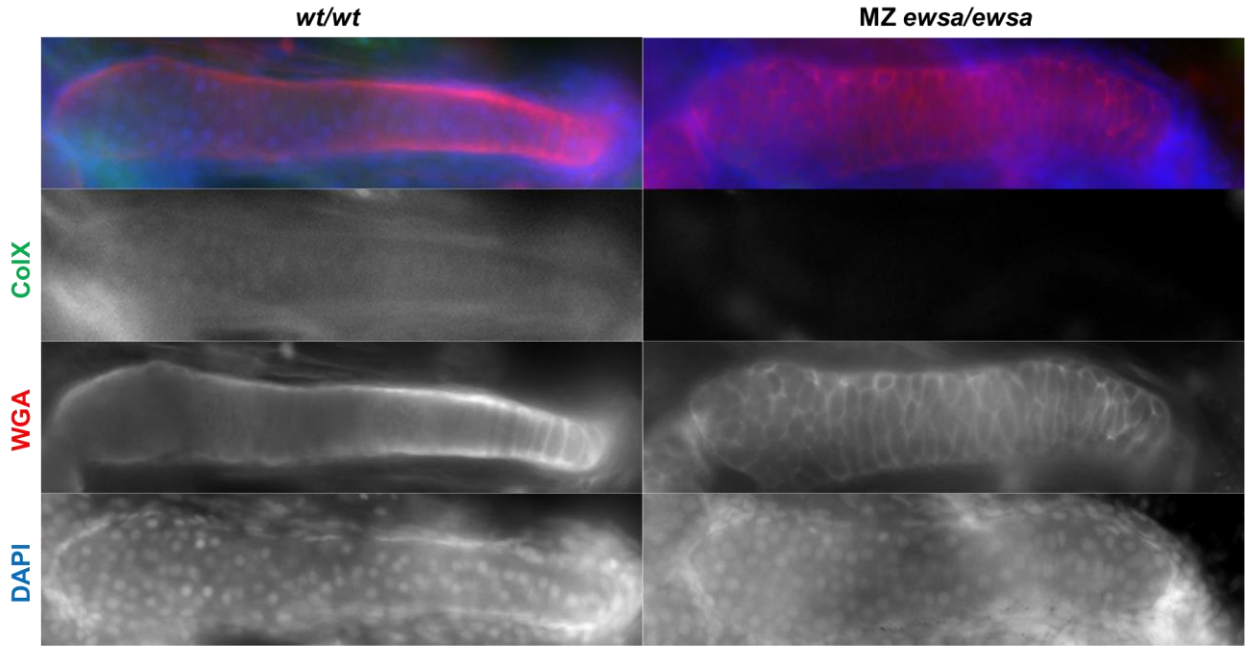

Figure 22. Collagen10a1 expression is decreased in ceratohyal of MZ *ewsa/ewsa* mutant embryos compared to *wt/wt* at 5dpf. Ventral views of ceratohyal of 5dpf *wt/wt* and MZ *ewsa/ewsa* mutant embryos (anterior to left) visualized by immunohistochemistry using anti-Collagen10a1 antibodies (green) and cartilage stain WGA (red). 1:100 antibody dilution.

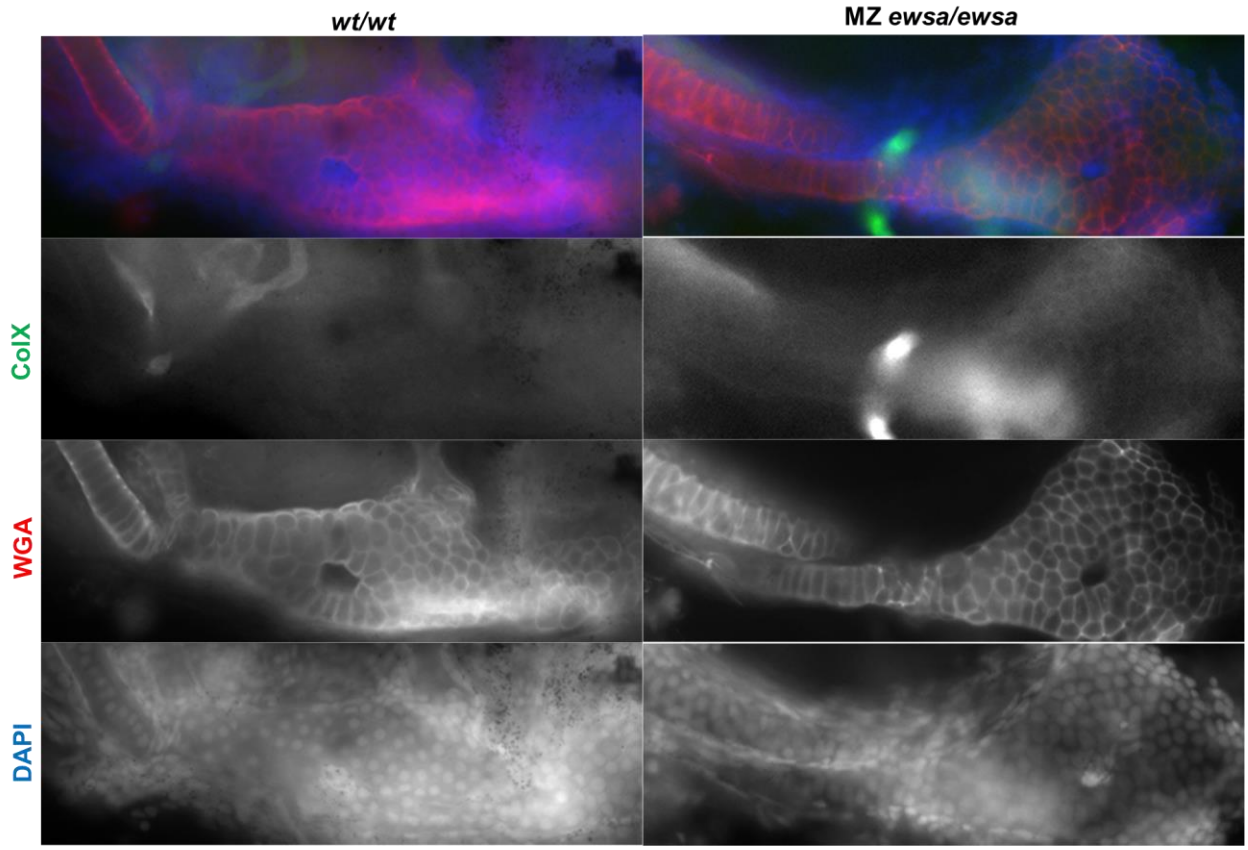

Figure 23. Collagen10a1 expression is similar in hyomandibular of MZ *ewsa/ewsa* mutant embryos compared to *wt/wt* at 5dpf. Ventral views of ceratohyal of 5dpf *wt/wt* and MZ *ewsa/ewsa* mutant embryos (anterior to left) visualized by immunohistochemistry using anti-Collagen10a1 antibodies (green) and cartilage stain WGA (red). 1:100 antibody dilution.

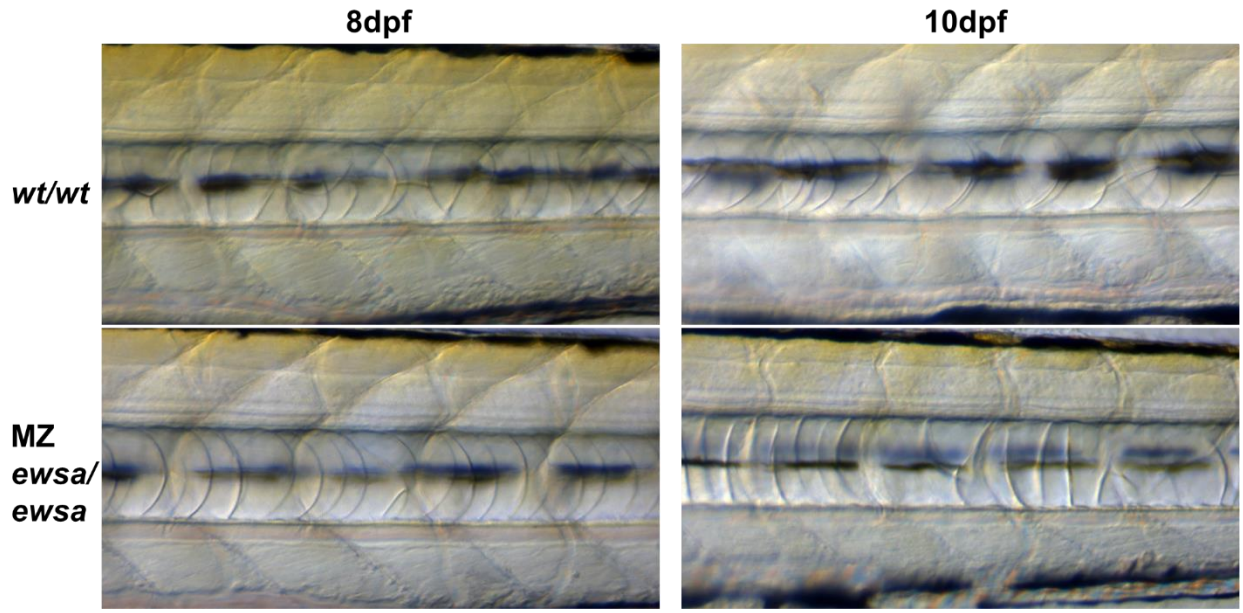

Figure 24. Notochord cells fail to intercalate in MZ *ewsa/ewsa* mutants compared to *wt/wt.* Brightfield analysis of the notochord cells of 8dpf and10dpf embryos. MZ *ewsa/ewsa* mutants show thicker notochord boundaries and fewer intercalated cells. Magnification 200x.